Brown University

DIVISION OF ENGINEERING

PROVIDENCE, R.I. 02912

HYDRIDING OF TITANIUM

First Annual Report (1996)

Contract No. N00014-96-1-0272

DISTRIBUTION STATEMENT A

Approved for public release;
Distribution Unlimited

HYDRIDING OF TITANIUM

First Annual Report (1996)

Contract No. N00014-96-1-0272

Submitted to
The Office of Naval Research
800 N. Quincy Street
Arlington, Virginia 22217

Submitted by
Clyde L. Briant, K. Sharvan Kumar, and Zhengfu Wang
Division of Engineering
Brown University
Providence, Rhode Island 02912

DTIC QUALITY INSPECTED 2

19970324 061

DISTRIBUTION STATEMENT A
Approved for public release;
Distribution Unlimited

TABLE OF CONTENTS

ABSTRACT

This report presents a summary of the first year of work on ONR Contract N00014-96-1-0272, Hydriding of Titanium. The overall goal of this project is to evaluate the performance of grade II titanium in sea water applications. The reason for undertaking this work is that the US Navy would like to use titanium in a number of critical applications, where it would come in contact with sea water at elevated temperatures. Although the general reputation of titanium is that it is quite corrosion resistant in these environments, there is the possibility that it could pick up sufficient hydrogen from this environment to become hydrided and thus lose its mechanical integrity.

The work done in the first year of this program has addressed the following issues.

- A literature survey has been conducted on the behavior of grade II titanium in sea water applications.
- The corrosion potential of grade II titanium has been measured as a function of temperature, pH, and salt concentration.
- Mechanical tests have been performed which determine the change in ductility of grade II titanium as a function of electrochemical potential, pH, strain rate, and sample geometry.
- The effect of galvanic coupling on the corrosion potential of grade II titanium and its ability to form hydrides has been investigated.

The results that we have obtained generally verify the good response of grade II titanium for this application that has been reported in the literature. Hydrides can form on the surface of the sample at potentials below approximately -600mV_{SCE}. However, these hydrides do not seriously degrade the mechanical properties of this material, and the samples showed good ductility even for tests run at electrochemical potentials as low as -1400 mV_{SCE}. When a thick hydride layer was formed on the surface by extreme cathodic charging, only a small decrease in elongation could be observed; even though the brittle film cracked, the underlying metal was ductile. An increase in temperature and a decrease in pH increased the electrochemical potential of the titanium. Galvanic coupling experiments showed that hydrides formed in titanium coupled to zinc and aluminum at all temperatures between 23 and 90°C. The reaction with zinc was so extreme that the zinc dissolved from the couple. When the titanium was coupled to HY80 steel, hydrides formed when the temperature exceeded 70°C. It would appear, based on the above results, that the main concern would be applications where galvanic coupling might occur between the Navy steel HY80 and grade II titanium. Over long periods of time, brittle hydrides could form and crack, leading to very slow crack propagation.

1.0 INTRODUCTION

This report presents a summary of the first year of work on ONR Contract N00014-96-1-0272, Hydriding of Titanium. The overall goal of this project is to evaluate the performance of grade II titanium in sea water applications. The reason for undertaking this work is that the US Navy would like to use titanium in a number of critical applications, where it would come in contact with sea water at elevated temperatures. Examples would include condensers and heat exchangers in which sea water is used as a coolant. Although the general reputation of titanium is that it is quite corrosion resistant in these environments, there is the possibility that it could pick up sufficient hydrogen from this environment to become hydrided and thus lose its mechanical integrity. As cited below, a few such cases have been reported in the literature.

During the first year of work the goals of the project have been the following:

- To carry out a thorough literature survey to obtain all available information about the conditions under which titanium will absorb large quantities of hydrogen from exposure to seawater.
- To make measurements of the corrosion potential under different conditions
- To define regions of electrochemical potential, temperature and solution acitivity which would most likely cause hydrogen absorption by the metal.
- To examine the effect of galvanic coupling on the corrosion potential and the propensity of titanium to form hydrides.

All of this work has now been completed and the results are contained in this document. The report will be organized in the following way. First we will present a literature survey of the behavior of titanium in sea water. We will then present the results of this investigation. Finally, we will present our plans for the second year.

2.0 LITERATURE REVIEW

In general, titanium is viewed as very resistant to corrosion in sea water environments. A number of publications (1-7) published by various manufacturers of titanium strongly urge its use for such applications. For example, TIMET Corporation reports(2) that unalloyed titanium corrodes at a maximum rate of 4×10^{-5} mm/year over a range of depths into the ocean. However, these documents also point out three areas of concern. One is that titanium can undergo crevice corrosion in this type of environment. The second is that if titanium picks up hydrogen from this environment it can form hydrides, which in turn limit the ductility of the material. The third, which relates to the second, is that if titanium becomes galvanically coupled to another metal, it will usually be the cathode and will absorb the hydrogen that is generated. Furthermore, as shown in Figure 1, if the relative areas of the anode and cathode are not properly balanced, the corrosion of the other metal can be significantly enhanced.

The more detailed reports on the behavior of titanium in sea water can be divided into two groups of studies. The first of these includes results of laboratory studies. These results provide much useful data that help us to predict the behavior of titanium in engineering applications. The reason for carrying out much of this research was to determine how titanium would perform in desalination plants. The other set of studies are analyses of field data. Much of this information also comes from desalination plants, although other applications have been examined. We now present a summary of these two types of studies. We focus primarily on the possibility of the titanium absorbing hydrogen and the effect of the hydrogen on mechanical properties, since the corrosion behavior of titanium in this environment appears to be quite good, provided crevices can be avoided.

2.1 Laboratory Studies

Laboratory studies on the hydrogen embrittlement of titanium in sea water environments have established some basic trends. The results reported here are all for commercial purity titanium, similar to grade II.

Figure 2 shows the hydrogen concentration plotted as a function of electrochemical potential (8). Hydrogen is first absorbed at a potential of approximately $-700mV_{SCE}$ and increases extremely rapidly with decreasing potential. These results correlate well with the polarization curve for titanium in sea water (9) shown in Figure 3. This figure shows that as the potential decreases, the cathodic reaction changes. In the region between $-700mV_{SCE}$ and $-1400mV_{SCE}$, the cathodic reaction is the reduction of hydrogen and below this potential the cathodic reaction is reduction of water. In either case atomic hydrogen is generated and

can be absorbed by the titanium. The data in Figure 2 are replotted in Figure 4 to include results taken from another study (10) in which the electrochemical potentials employed were below the electrochemical potentials where the reduction of water should be the primary cathodic reaction. Also note that the temperature in these latter tests was lower. However, these results yield a good extrapolation to those shown in Figure 2.

Galvanic coupling can change the corrosion potential of titanium and affect hydrogen absorption (8,10,11,12), as the data presented in Figure 5 demonstrate. Samples coupled with zinc and iron showed significant hydrogen pick-up when exposed to sea water for a time of 720 hours, whereas titanium that was uncoupled or coupled to naval brass showed essentially no pick-up. The potential measurements, given in Table I, are consistent with the results shown in Figure 1. Specimens of uncoupled titanium and titanium coupled to naval brass have potentials above -750mV$_{SCE}$, whereas those for couples with steel and zinc are below this value. When compared with Figure 3 we would expect the latter two to show significantly more hydrogen absorption. Figure 5 also shows the importance of temperature on the amount of hydrogen absorption, as do results presented in Figure 6. It is clear that above about 100°C the amount of hydrogen absorbed greatly increases.

Table I
Corrosion Potential of Ti
Coupled with Other Metals
Deaerated 6%NaCl, pH6, T=100°C; Data taken from Ref. 8

Specimens	Ecorr (mV $_{SCE}$)
Ti	-350
Ti-Naval Brass	-500
Ti-Mild Steel	-800
Ti-Zinc	-1100

Two other important variables that affect hydrogen absorption by titanium are the pH of the solution and the surface finish. Figure 7 shows the results from two different studies (11,13) on the effect of pH on the amount of hydrogen taken up by the sample. The results shown in Figure 7a were taken from tests run in 3.5% NaCl in which the pH was varied by additions of acid or bases. The temperature of the solution was 90°C, the potential was -1900mV$_{SCE}$, and the test time was 1 hour. It is clear that in this short time test the hydrogen concentration decreases rapidly with increasing pH. The results (13) reported in Figure 7b were all obtained at room temperature, and different types of solutions (not all NaCl) were used to obtain the different pH values. Also, the charging

current density was set at 0.3mA/cm^2. Together these plots show the importance of decreasing pH on the amount of hydrogen absorption.

The effect of surface finish can have a significant impact on the amount of hydrogen absorbed when titanium is exposed to sea water. Figure 8 plots the hydrogen concentration as a function of applied potential for samples that either had a cleaned surface or samples which had surfaces oxidized at either 400 or 600°C. These results show that the oxide inhibits hydrogen absorption. Table II shows the hydrogen absorption when grade II titanium with different surface finishes was cathodically charged and also the effects on grade II titanium galvanically coupled to 2024 Al alloys. The results show that any kind of surface abrasion that would destroy the normally tenacious oxide of titanium tends to enhance pick-up of hydrogen. It has been noted, in particular, that abrasion of titanium in the presence of iron tends to enhance absorption of hydrogen, perhaps because hydrogen diffuses rapidly in iron through the oxide film (14). However, the results in Table II suggest that abrasion with an iron tool is no more deleterious than other methods that break down the oxide film.

Table II
The Effect of Surface Condition on Hydrogen Absorption
Data Taken From Reference 9

Sample	Surface Condition	Average Hydrogen Pick-up (ppm)
Grade II Ti*	Pickled Only	0
Grade II Ti*	Sandblasted-No Pickle	48
Grade II Ti*	Sandblasted and Pickled	16
Grade II Ti Coupled with 2024 Al**	Pickled Only	0
Grade II Ti Coupled with 2024 Al**	Sandblasted	44
Grade II Ti Coupled with 2024 Al**	Sandblasted and Vacuum Annealed	85
Grade II Ti Coupled with 2024 Al**	Surface Abraded with Iron	41
Grade II Ti Coupled with Fe**	Pickled Only	2
Grade II Ti Coupled with Fe**	Sandblasted and Vacuum Annealed	2
Grade II Ti Coupled with Fe**	Dented with a Ti Bar	4

*Cathodically charged at 9 mA/cm^2 for one hour at room temperature (-1900mV)
**Exposed to a boiling 3.5% ASTM sea salt solution with pH=8 for 500 hours.

Research has clearly shown that hydrides form in titanium (15-19). The most commonly observed hydride is δ hydride which, according to the phase diagram, would be in equilibrium with α-Ti and thus the first to form once the solubility limit is exceeded. It has a cF12 (CaF_2) structure and a composition of approximately $TiH_{1.05-2.0}$. ε-hydride forms at temperatures below 25°C at hydrogen concentrations of approximately 0.6 atomic percent. The chemical formula for this hydride is $TiH_{1.72-2.0}$ and it has a tI6 (ThH_2) structure. Reports (15,16) have also been published of a γ-hydride which forms at very low hydrogen concentrations. The stoichiometry is TiH_x with x less than one. As the hydrogen concentration increases, the γ-hydride disappears and is completely replaced by the δ-hydride. Many studies have not distinguished between these different types of hydrides but instead have relied simply on metallographic evidence to determine their presence. In the optical microscope, this phase is observed within the grains and has a lenticular or needle-shaped appearance; examples can be seen in Figure 39 presented later in this report. When the hydrides form by cathodic charging, they first form on the surface of the sample and then gradually penetrate into the material. Figure 9 shows the average thickness of the hydride layer in samples charged at the cathodic potential of -1600mV_{SCE} at 45°C. These results suggest that the hydride film tends to form rather quickly, but then progresses very slowly into the metal. The first layer of hydride thus appears to form a protective layer that inhibits further penetration of hydrogen. Results(20) suggest that hydrides first form when the hydrogen concentration exceeds approximately 30 ppm. Although the phase diagram suggests that the solubility should be on the order of 1000 ppm, the fact that the hydrogen is often concentrated at the surface and the chemical analysis probably measures a entire bulk sample explains this difference.

Evidence has been presented which shows that hydrogen in titanium can decrease elongation(18). The fracture that is produced is usually transgranular. However, the effects of cathodic charging on elongation and the hydride layer that results have been less well investigated. Jain and co-workers (21) have reported that grade II titanium tested in both acidic and alkaline brine suffers little, if any, decerase in elongation. Recent results by Simbi and Scully(22) indicate that the composition of the titanium can play an important role in determining the susceptibility of the titanium to hydrogen embrittlement resulting from cathodic charging. Their data are reproduced in Figure 10; the elongation to failure is plotted as a function of the oxygen equivalent in the material. This parameter is defined as

$$O^* = O + 2N + 2/3C \text{ (values in wt\%)} \qquad (1)$$

These results suggest that as the alloy becomes less pure, the damaging effects of hydrogen greatly increase. However, it should be noted that the increase in the oxygen equivalent causes the yeild strength to increase, which in most materials causes an increase in susceptibility to hydrogen embrittlement. Therefore, the mechanism by which the increased oxygen content exerts its effect is not clear.

2.2 Field Data

Although the laboratory data help us to understand the basic behavior of titanium in a sea water environment, nothing can take the place of field data which report the performance of the material in engineering applications over long periods of time. Fortunately, some data of this type exist for titanium and we now wish to summarize them.

Sato *et al.* (20) have monitored welded titanium tube in a test desalination plant and monitored its behavior. The results, presented in Table III, show that as the temperature increased, the amount of hydrogen absorbed by the metal increased. In particular, the end of one tube had an extremely high concentration of hydrogen. Hydrides were found in a number of the samples. The ductility was degraded in samples that had over approximately 500 ppm hydrogen, as shown in Figure 11.

Table III
Hydrogen Content in Welded Titanium Tubes Installed in a Test Plant
Data Taken from Reference 20

Section of Installation	Brine Temperature (°C)	Hydrogen Concentration (ppm) in 2000 h. Exposure-Samples Not Pickled		Hydrogen Concentration (ppm) in 8800 h. Exposure-Samples Pickled in HCl	
		Middle of Tube	End of Tube	Middle of Tube	End of Tube
Brine Heater	105-120	150	350	560	870
Evaporator	89-98	170	230	260	270
Evaporator 4	75-82	70		260	
Evaporator 6	59-66	110		140	
Evaporator 8	42-50	52	120	140	110
Evaporator 10	24-33	70		130	

Because these results showed that large amount of hydrogen could be absorbed, Sato *et al.* (20) carried out tests in autoclaves that simulated as closely as possible the conditions that would exist in the desalination plant. This allowed them to monitor certain parameters more accurately. The results are summarized in Table IV, and several important points should be noted. The electrochemical potential ranged between -700 to +200mV$_{SCE}$ for samples that were not galvanically coupled. Such variation presumably arises from

differences in surface finish and also from variations in the way the solution interacts with titanium. Galvanic coupling of titanium also has a significant effect on the electrochemical potentials that can be obtained. For example, these authors reported that if titanium was galvanically coupled to stainless steel, the potential could vary between -600 to -800mV_{SCE}, whereas if the titanium was coupled to naval brass the potential varied between -500 to -600mV_{SCE}. The hydrogen contents absorbed during the test are somewhat less than those actually reported from the plant exposure. Hydrides were observed in samples with hydrogen concentrations greater than approximately 30 ppm. It should also be noted that these hydrides were observed in samples that had impressed potentials of -1100mV_{SCE}.

The remaining plant data for titanium in sea water environments tends to be observations of the behavior of the material in certain applications. Near room temperature titanium has shown excellent performance in sea water (23,24). Examples of these applications include construction of a deep water gravity tower (25), riser connectors in ocean platforms (26), doors on diving bells, construction of compression chambers, and construction of submersible chambers (6). Examples are referred to where titanium has been used in sea water applications for thirty years with no incidence of environmental failures.

Table IV
Results for Titanium Samples Exposed in an Autoclave to Simulate High Temperature Sea Water
Data Taken from Reference 20

Specimen	pH	Duration of Test (hr.)	Electrochemical Potential (V_{SCE})	Hydrogen Concentration (ppm)	Hydrides Observed
Ti	8.1-8.7	624	-0.21 to -0.75	21	No
Ti	8.1-8.7	172	-0.5 (impressed)	27	No
Ti	8.1-8.7	120	-1.1 (impressed	33	Yes
Ti	5.0-9.2	720	0 to -0.5	18	No
Ti	5.0-9.2	720	-1.1 (impressed)	50	Yes
Ti	3.6	100	-0.06 to -0.3	17	No
Ti	3.6	100	-1.1 (impressed	30	Yes
Ti	5.1-8.5	1500	0.2 to -0.4	22	No
Ti-Naval Brass	8.1-8.7	624	-0.485 to -0.655	25	No
Ti-Steel	8.1-8.7	624	-0.695 to -0.790	21	No

Table V
Summary of Service Performance of Titanium in Sea Water at Temperatures Above Ambient

Application	Conditions	Performance	Reference
Sour water tube failure	Severely abraded tube, galvanically coupled with 304 stainless steel, 120°C.	Failure resulting from hydriding	20
MEA Regenerator Overhead Condenser	Galvanic couple with carbon steel in the presence of H_2S. Temperature above 110°C.	Failure resulting from hydriding	27
Titanium heat exchanger for caustic pulping liquor	Temperature above 165°C	Failure after three years of operation resulting from hydrogen embrittlement	27
Heat Exchangers in St Croix Desalination Plants	Brine waters; highest temperature 235°F.	Out of over 5000 tubes, two were leaking after seven years from vibration induced fretting; in the second plant 8 were leaking after one year from faulty installation	28
Florida Power and Light Company Condenser Tube	T~45°C, unit under cathodic protection so that electrochemical potential was less than -1V_{SCE}	Hydrides observed	10
Corrosion testing system constructed of Ti	Equipment saw a variety of conditions with saline water. Attack occurred in areas where T>100°C and pH<8.7	Crevice corrosion and hydrides observed	29
15 Stage Desalination Plant	Used 100 miles of seamless Ti tubing throughout plant	No observable corrosion or problems	30
Multi-Stage Flash Desalination Plant	Titanium condenser. Attack occurred after four months where temperature of salt water was 88 to 110°C.	Crevice corrosion and hydrides	31

However, at elevated temperatures evidence of hydriding and observations of part failures have been recorded. These are summarized in Table V. The entries in this table were

chosen specifically to include examples where enough information was given so that one could compare the results with laboratory data. As a result of these types of failures, general rules have been developed (1-3) to described conditions under which cracking will occur. They are the following:

(1.) Failure can result if the pH of the solution is less than three or greater than 12 or the metal surface has been damaged by abrasion.

(2.) Failures and hydriding can occur more easily if the temperature of the solution is greater than 80°C. At lower temperatures, surface hydrides will form but experience indicates that these will not seriously affect mechanical properties of the metal, since failures resulting from hydride formation are rarely encountered below this temperature.

(3.) There must be some mechanism for generating hydrogen. This may be a galvanic couple, cathodic protection by impressed current or dynamic abrasion of the surface with sufficient intensity to depress the metal potential below that required for spontaneous evolution of hydrogen.

(4.) If crevices are present, they can cause corrosion.

One of the goals of this ONR program is to determine the general validity of these guidelines and whether or not they apply to all situations. As a caveat, it should be noted that some of the failures reported in Table V occurred because of mishandling of the titanium, and thus these rules may be overrestrictive.

3.0 EXPERIMENTAL PROCEDURE

3.1 Material

The material used was commercially pure grade 2 titanium in the form of 1.12mm thick rolled sheet. It was used in the as-received condition (749 °C, 3 minutes and air cooling). Its chemical composition and mechanical properties, as reported by the manufacturer, are shown in Tables VI and VII, respectively.

Table VI
Chemical Composition of Titanium

Element	Oxygen	Carbon	Nitrogen	Iron
Weight %	0.14	0.02	0.008	0.08

Table VII
Mechanical Properties of Titanium

Yield Strength (MPa)	Ultimate Tensile Strength (MPa)	Elongation (%)
344.5	506.7	28

3.2 Electrochemical Measurements

Electrochemical measurements, including the corrosion potential and the polarization curve, were carried out at room temperature (23°C), 50°C, 70°C and 90°C in solutions of 6%NaCl (pH=1 and pH=5.5) and sea water (pH=8) (32). The specimens were in the form of a square, 10 mm on a side, with 1 cm^2 of surface area exposed to the solution. Before testing, the specimen surface was abraded with 600-grit silicon carbide paper. The potential was controlled with reference to a saturated calomel electrode (SCE). For corrosion potential measurements, the specimen was held at -1400 mV_{SCE} for 3 minutes to remove the surface oxide film. Then the potential control was cut off; after 2 minutes, the value of the corrosion potential was measured. The measurements continued to be taken as a function of time for up to about 120 minutes. For polarization curve measurements, the specimen was held at -1400 mV_{SCE} for 3 minutes to remove the surface oxide film, allowed to sit at the free corrosion potential for 3 minutes, and then scanned from -1800 mV_{SCE} to the free corrosion potential at the rate of 10 mV/min.

To measure galvanic corrosion, titanium was coupled with monel, inconel, naval brass, 316 stainless steel, navy steel HY80, five-nines aluminum, 6061 aluminum and

zinc. The titanium sample has a square shape with a side length of 16 mm and a round hole in the center with a diameter of 6.5 mm. The metal to be coupled with the titanium had a cylindrical shape of slightly larger diameter than that of the hole. It was forced into the hole to make galvanic contact. The corrosion potential for coupled samples was measured under the same conditions listed above. In addition, samples of titanium coupled with HY80 steel and zinc were exposed for one week to a solution of 6%NaCl (pH=1) at room temperature, 50°C, 70°C, or 90°C. A series of titanium samples was charged under different applied potentials from -200 mV_{SCE} to -1400 mV_{SCE} in 6% NaCl (pH=1) solutions at 70°C for 24 hours.

3.3 Mechanical Tests

Three types of specimens were used for the mechanical tests. All were sheet specimens. The specimen designated as type A had a smooth gauge length of 31.75 mm and that designated as Type B had a smooth gauge length of 12.7 mm. Both had gauge widths of 6.35 mm. Another set of samples contained a notch 2.54 mm deep subtending an angle of 60° filed into the center of one edge of each of the test pieces. The specimens were cut from an as-received sheet with the length perpendicular to the rolling direction and machined to the required size. The center part of the specimen was polished with 600-grit silicon carbide paper and degreased with acetone before testing. One set of tests were performed by straining a type A specimens in air after prior cathodic hydrogen charging with an applied current density of 0.5 A/cm^2 in 6%NaCl (pH=1) solution at 70 °C. Type B specimens and the notched specimens were tested while immersed in the charging solution at 70 °C under potential control. Figure 12 shows the setup for mechanical tests. For dynamic hydrogen charging mechanical tests, the specimen was coated with silicone except near the center section. This part was under potential control. At the start of the test, it was held at -1400mV_{SCE} for 3 minutes after the required temperature was reached, and then it was held at the required applied potential for the remainder of the test. The specimen was then strained slowly to failure at crosshead speeds of 0.25 mm/min, 0.07 mm/min, $7x10^{-3}$ mm/min and $7x10^{-4}$ mm/min using an Instron tensile testing machine. For comparison, mechanical tests in an inert oil were conducted at the same temperatures and crosshead speeds. Susceptibility to environmental cracking (SCC) was discerned from the ratio of the elongation-to-fracture in solution to the elongation-to-fracture in oil.

3.4 Fracture Surface Examination and Hydride Detection

The fracture surface was cut from the specimen after failure and cleaned ultrasonically in acetone. The fracture morphologies were examined by scanning electron

microscopy (SEM). After testing, the specimen was sectioned along the loading direction, ground and polished to 1 μm. Hydrides were revealed by etching the specimen in a mixture of 285 ml H_2O + 5 ml HNO_3 + 10 ml HF mixture. Hydride film features and thicknesses were examined by SEM. Hydrides were also detected by X-ray diffraction (XRD), which was performed using Cu-Kα radiation (40KV, 35mA) in all experiments.

4.0 RESULTS AND DISCUSSION

4.1 Electrochemical Measurements

The corrosion potentials for grade 2 titanium in 6%NaCl solution (pH=1 and pH=5.5) at different temperatures are shown in Figure 13. The corrosion potential was lowest at room temperature and increased with increasing temperature. At each temperature, the corrosion potential in the solution with a pH value of 1 was higher than that in the solution with a pH of 5.5. The scatter in these measurements was ±25mV. The measured value of the corrosion potential depended on testing time. The values shown in Figure 13 were obtained after 3 minutes of cathodic polarization at -1400 mV_{SCE} and then 2 minutes at the free corrosion potential. Figures 14 and 15 show the variation of the corrosion potentials with testing time for grade 2 titanium in 6%NaCl solution with pH values of 1 and 5.5, respectively. On these curves the zero time point corresponds to the values in shown in Figure 13. For the solution with a pH value of 1, the corrosion potential generally increased with increasing time at each temperature and reached a stable value after about 120 minutes. Although the specimen surface was abraded and cathodically charged for 3 minutes, an oxide film could still form on its surface in solution, and the formation of the film was probably responsible for the increase of the corrosion potential. For the solution with a pH value of 5.5, the corrosion potential tended to decrease slightly after it reached its maximum at room temperature and 50°C. One observation that was made during the measurement of the corrosion potential was that there could be some scatter in the corrosion potential values measured after several hours. This variation could range over several hundred millivolts and is consistent with the ranges listed in Table IV.

Both the temperature and the pH value had an influence on the corrosion potential, which is defined as the point where cathodic reaction rate equals the anodic reaction rate. For titanium in 6%NaCl solution with a pH of 5.5, the surface of the sample was covered by an oxide film; the dissolution rate of the sample was small due to the oxide film and changed very little, even though temperature increased. However, the cathodic reaction process on this surface was greatly increased by the increased temperature, resulting in the increase of the corrosion potential. Thus, from the results in Figure 13, it could be deduced that the cathodic process was enhanced by an increase in the temperature of the solution with a pH value of 1. It has been reported that the oxide film on titanium is unstable and dissolves at pH values below 3 and above 12 (9). A surface film could decrease anodic dissolution rate, but our results show it did not retard hydrogen evolution.

Commercially pure grade 2 titanium has been widely used in sea water (23,24,33,34). Figure 16 shows the corrosion potential in synthetic sea water with a pH

value of 8 at different temperatures. Similar to the results in 6%NaCl solution, the corrosion potential in sea water increased with increasing temperature. Higher temperatures would result in rapid oxidation on the specimen surface.

Figures 17 and 18 represent the polarization curves for grade 2 titanium at different temperatures in 6%NaCl solution with pH values of 1 and 5.5, respectively. In the acidic solution (pH=1), the main cathodic process usually is hydrogen evolution; at room temperature the cathodic process at all potential ranges was controlled by the hydrogen evolution reaction; however, due to the large solubility and high diffusion rate of oxygen in aqueous solutions at high temperatures, the cathodic process was controlled by the oxygen adsorption reaction at the potential between 180 to -700 mV_{SCE} at 50°C and 70°C, and between 100 to -350 mV_{SCE} at 90°C. The hydrogen liberation rate at 90°C was much higher compared to other temperatures. It is not clear why the cathodic reaction rate kept constant at potentials between -1000 to -1600 mV_{SCE} for the curves at room temperature, 50° and 70°C, and between -600 to -1200 mV_{SCE} for the curve at 90°C. The further increase in the cathodic reaction at lower potential indicated another cathodic process commences; see Figure 2.

In the solution with a pH value of 5.5, the oxygen adsorption reaction played a dominant role over applied potentials from the free corrosion potential to -1200 mV(SCE) at all temperatures. The cathodic reaction rate or hydrogen liberation rate was small compared to the value in acidic solutions at the same temperatures. It has been reported that surface oxidation does not retard hydrogen evolution (12). Therefore, the increase of pH value in this solution was responsible for the decrease of the cathodic reaction rate in this solution.

In both testing solutions, the free corrosion potential measured by the polarization curve increased with increasing temperature, which was consistent with the corrosion potential measurements at different temperatures shown in Figure 13. However, the corrosion potential values were different for the two testing methods. The corrosion potential determined from the polarization curve was much higher than that from the direct corrosion potential measurement, a result often observed in electrochemical tests. The corrosion potential can be influenced by many factors including species in solution, concentration, pH, temperature, surface condition, etc. To determine the polarization curve, the sample was scanned from -1800 mV_{SCE} to the free corrosion potential. The surface condition was changed during the scan, and this change in the surface condition probably led to the difference in the potential measured by the two methods. It can be concluded that both the increase of temperature and the decrease of pH value in solution increased the cathodic reaction rate more strongly than the anodic reaction rate, resulting in the increase

of corrosion potential value. Figure 19 shows the cathodic polarization curve for grade 2 titanium in sea water with a pH value of 8. Higher temperatures increased both corrosion potential and cathodic reaction rate. The results were similar to that in 6% NaCl with a pH=5.5.

4.2 Titanium Coupled With Other Metals

When two dissimilar metals are connected electrically in a conducting solution, a current flows between the two because of dissimilar electrochemical potentials. The metal with the more negative potential becomes a cathode and is protected from corrosion, and the metal with the more positive electrochemical potential becomes the anode. The current flowing between the two metals accelerates the dissolution of the anode. In our experiments the measured corrosion potential for the couple is actually a mixed potential between titanium and the other metal coupled with it and depends upon the corrosion potential of this metal under the same testing conditions. When titanium acts as an anode, the dissolution is not accelerated significantly because of the oxide film on its surface. When titanium acts as a cathode in the couple, hydrogen is evolved on the titanium surface due to the corrosion of the less noble material, and it is possible for hydride formation or hydrogen embrittlement to occur.

The corrosion potentials were measured for titanium galvanically coupled with a number of metals including monel, naval brass, 316 stainless steel, inconel, HY80 navy steel, five-nines aluminum, 6061 aluminum and zinc. Figures 20 and 21 show the corrosion potentials for titanium coupled with these metals in 6%NaCl solution at different temperatures and different values of pH.

In the solution with a pH value of 1, the corrosion potentials for titanium coupled with naval brass, monel and inconel were higher than uncoupled grade 2 titanium. The titanium coupled with naval brass had the highest corrosion potential, and next was the titanium coupled with inconel. This difference was obvious at room temperature and became less at high temperatures. Naval brass, monel and inconel caused titanium to become an anode. The corrosion potentials for titanium coupled with HY80 steel and 316 stainless steel were higher than grade 2 titanium at room temperature, but became lower than the value for uncoupled titanium at high temperatures. In these couples titanium became an anode at room temperature and a cathode when the temperature was increased; however, the potentials for the two dissimilar metals were close, and the driving force for this galvanic corrosion was small. Five-nines aluminum and 6061 aluminum had nearly the same electrochemical behavior in this solution. The corrosion potential for titanium coupled with these two metals was approximately $-800mV_{SCE}$ and changed little with increasing

temperature. Titanium became a cathode when coupled with these two metals. Titanium coupled with zinc had a corrosion potential of about -1075mV_{SCE} for all temperatures and was the cathode of the pair. The couple produced strong hydrogen evolution from the titanium surface, and zinc rapidly dissolved in this solution.

In the solution with a pH value of 5.5, the corrosion potentials for titanium coupled with other metals were similar to those in the solution with a pH value of 1. One exception was the titanium coupled with monel which had a corrosion potential lower than grade 2 titanium at 50°C and 70°C in the pH 5.5 solution.

The corrosion potentials for the galvanic couples described above were the values taken after 3 minutes of cathodic polarization at -1400 mV(SCE) and then 2 minutes at the free corrosion potential. The corrosion potential values varied with time. In the most cases, they reached a stable value after about 120 minutes, which meant a stable oxide film formed on the specimen surface. Table VIII shows the final corrosion potential values for titanium galvanically coupled with a number of metals.

Table VIII
Corrosion Potentials for Ti Coupled with Different Metals After 3min. and120min.
Top Entry is 3 Min.; Bottom Entry is 120 min.;Values are in mV_{SCE}

Sample	Ti-Monel			Ti-Inconel			Ti-Zinc		
Temperature (°C)	23	50	70	23	50	70	23	50	70
pH=1	-446 -258	-403 -257	-365 -325	-365 -295	-365 -260	-382 -365	-1015 -1025	-1035 -1028	-1003 -993
pH=5.5	-550 -255	-521 -275	-490 -365	-621 -200	-456 -160	-410 -260	-1063 -1089	-1095 -1093	-1072 -1082

For comparison, the corrosion potentials for titanium coupled with the same metals were measured in synthetic sea water with a pH value of 8 at different temperatures. Figure 22 shows the results of these measurements. Similar to the results in 6%NaCl solution, the naval brass and monel caused titanium to become an anode; however, inconel caused titanium to become a cathode. The behavior of inconel was nearly the same as 316 stainless steel. HY80, five-nines aluminum, and 6061 aluminum became anodes at each temperature when coupled with titanium. Titanium was the cathode when it was coupled with zinc in synthetic sea water.

Titanium is the cathode in many of the couples described above, which means that hydrogen is evolved on the titanium surface due to sacrificial corrosion of the less noble material. The reaction rate for hydrogen evolution is strongly dependent on the corrosion potential value for the coupled sample. Covington (9) indicated that hydrogen absorption occurred in natural sea water only when titanium had a potential lower than approximately

occurred in natural sea water only when titanium had a potential lower than approximately -700mV_{SCE}. Fukuzuka (11) reported a limiting potential for hydrogen absorption of -750mV_{SCE} in aerated sea water at 25 °C and -650 mV_{SCE} in deaerated sea water at 100°C. Sato (12) also reported that the limiting potential for hydrogen absorption was -750 mV_{SCE} in natural sea water. The amount for hydrogen absorption also is dependent on the potential. Experiments by Nosetani (35) in artificial sea water at ambient temperature showed that no hydrogen absorption was detected after three months at a potential of -600 mV_{SCE}, 20 ppm were detected after exposure at -800 mV_{SCE}, and 100 to 200 ppm after exposure at -1000 to -1200 mV_{SCE}. Experiments by Schutz and Grauman (10) indicated that significant hydriding of titanium in neutral sea water only occurred at potentials lower than -1200 mV_{SCE}. They proposed a limit of -1000 mV_{SCE} for avoiding significant hydriding of titanium in sea water below 45°C (10).

Therefore, for the metals in these experiments, naval brass, monel, inconel and 316 stainless steel would not be expected to absorb hydrogen in sea water because their corrosion potentials are higher than -650 mV_{SCE}. Navy steel HY80, 6061 aluminum, and five-nines aluminum could cause hydrogen evolution in sea water if they were coupled with titanium. However, the corrosion potentials were just around -750 mV_{SCE}, and the amount of hydrogen absorption should be very low; for example, it should be about 20 ppm at -800 mV_{SCE} after three months in artificial sea water (35). This would not cause a significant problem for application of grade 2 titanium based on the mechanical tests reported in the later section. Zinc certainly could cause large amount of hydrogen absorption in natural sea water.

4.3 Exposure Tests

In 6%NaCl solution, the corrosion potentials for titanium coupled with HY80 steel and 316 stainless steel were higher than grade 2 titanium at room temperature, but lower than its value at high temperatures. Because of its importance to the Navy, titanium coupled with navy steel HY80 was chosen for an exposure test. The titanium/zinc couple was also chosen for this test because it developed the most negative electrochemical potential. The coupled samples were exposed in 6%NaCl solution (pH=1) at different temperatures for one week.

When samples of titanium coupled with navy steel HY80 were exposed in solution at room temperature and 50 °C, no hydrogen evolution could be observed with the naked eye, but the intensity of hydrogen evolution increased with increasing temperature. Significant hydrogen evolution could be observed from the surface of titanium coupled

with zinc, even at room temperature. Zinc dissolved in the solution and disappeared after one week exposure in the solution at room temperature and after one day exposure at 90°C.

4.4 X-Ray Diffraction

X-ray scans were made over a small range of angles, from 34° to 45°. This range should include peaks from both δ- and γ-hydrides, the two most likely to occur in these tests. Figures 23 to 26 show the X-ray diffraction results for titanium coupled with the navy steel HY80 exposed to 6%NaCl solution with a pH value of 1 for one week at different temperatures. Experiments indicated that no hydrides could be detected at room temperature and no obvious hydride could be detected at 50 °C. The hydrides γ -TiH and δ-TiH_2 could be detected from the titanium surface exposed to solution at 70°C and 90°C. Temperature increased the critical potential for hydrogen evolution and increased hydrogen evolution rate as well.

Figures 27 to 30 show the XRD results for titanium coupled with zinc and exposed to 6%NaCl solution (pH=1) for one week at different temperatures. For these experiments, hydrides could be found on the titanium surface at any testing temperature. Although the sample for titanium coupled with zinc had a very low corrosion potential compared to titanium coupled with the navy steel HY80, the peak strength of the hydride for titanium coupled with the zinc sample was not much stronger than titanium coupled with the navy steel HY80. This result can be easily understood if one compares the details of the tests. The Navy steel-Ti couple was exposed for the complete seven day test. However, in the zinc test, the zinc disappeared in five days after the sample was exposed to the solution at room temperature, in two days at 50°C and in one day at 70°C and 90°C. Even though the Ti was left in solution for the full seven days, hydrogen evolution stopped once the zinc was dissolved and the Ti presumably returned to its corrosion potential.

In order to obtain the relationship between hydride formation and the applied potential, the grade 2 titanium samples were charged in 6%NaCl solution (pH=1) for 24 hours at 70°C under the control of applied potential from -200 mV_{SCE} to -1400 mV_{SCE}. The samples were examined by XRD after being charged at a control potential in solution. Figures 31 to 38 show the XRD results for these experiments. From -200 mV_{SCE} to -600 mV_{SCE}, XRD results (Figures 31-33) gave nearly the same pattern; no hydride was detected in this range of potential. Hydrides were first observed at a potential below -700 mV_{SCE}. Hydrogen evolution was obviously observed by the unaided eye at the potential of -800 mV_{SCE} and below.

It should be noted that at a potential of -600 mV_{SCE} the sample was slightly cathodic relative to the corrosion potential of uncoupled titanium. However, no hydrogen evolution was observed and no hydrides detected. However, the titanium coupled with HY80 steel formed hydrides at the same potential. Therefore, we conclude that with sufficient time hydrides will form at this potential and we conclude that -600mV_{SCE} probably represents the cut-off potential above which hydrides will not form.

It was concluded that the potential for hydride formation was about 100 mV_{SCE} lower than corrosion potential at the testing condition. The amount of hydride was dependent on cathodic overpotential and potential charging time.

4.5 Hydride Examination

Figure 39 shows the microstructure of the hydrides from the specimen which was cathodically charged charged in 6%NaCl solution with current density of 0.5A/cm^2 for 12 hours. Hydrides formed on the titanium surface and penetrated into the titanium matrix and had a needle-shaped appearance. The thickness of the hydride layer varied with testing conditions; for example, temperature, pH value, chemicals, applied potential or current density and hydrogen charging time. All hydrides were found to form on the titanium surface; no hydrides were found in the interior of metal after hydrogen charging, consistent with the report that no appreciable diffusion of the hydrogen in alpha titanium occurs at temperatures below 80°C (36).

4.6 Mechanical Behavior

There are several ways in which hydrogen affects the mechanical properties of titanium (37). First, hydrogen can react with the metal to form a discrete hydride phase which is brittle and has very different elastic properties from the parent lattice. Second, hydrogen can interact with dislocations and internal cracks, affecting plastic behavior. Finally, it can diffuse monatomically to pores or cracks in the lattice and recombine to form bubbles and gas pockets. For titanium and its alloys, hydride formation and cracking are the main causes of failure. Hydrides formed both in the interior of the metal and at the surface will decrease the plasticity of the material. There are two ways for hydrogen to enter the material. One is internal hydrogen trapped during casting or a high temperature solution treatment, which to some extent can be controlled. Another is hydrogen picked-up from environments in which titanium is being used. This type of hydrogen entry may be more difficult to avoid. The experiments performed in this study examine the effect of environmental hydrogen on the mechanical properties of the material.

Smooth specimens (type A) were cathodically charged in 6%NaCl solution at 70°C with a current density of 0.5A/cm^2 for various periods of time and then tested in tension in air. Microstructural examination indicated that a hydride film covered the specimen surface. X-ray diffraction confirmed that hydrides were present in these samples. Tensile samples were pulled to failure at a crosshead of 0.25 mm/min. Although the yield and ultimate tensile strengths of the samples were unaffected by the hydrogen charging, the elongation decreased. Figure 40 shows the ratio of the elongation-to-fracture after hydrogen charging to the elongation-to-fracture in air without hydrogen charging. The elongation decreased with increasing hydrogen charging time, but the effect was not great. Examination of the fracture surface of the charged samples showed that the center of the sample failed in a ductile manner but that there was a rim of brittle fracture on the outer edge. Figure 41 shows the appearance of the fracture surface.

Hydrides formed on the specimen surface during hydrogen charging; there were no hydrides in the interior of metal. The effect of hydrogen on the mechanical properties came from the surface hydride film. Figure 42 shows that the hydride film thickness increased with increasing hydrogen charging time. The hydride film is brittle and has very different elastic properties from the parent lattice, and the film broke when the specimen was tested in tension. Figure 43 shows the appearance of a surface hydride film after yielding of the specimen. Many small cracks are seen on the surface. However, the surface layer of the hydride had little effect on the mechanical properties of titanium after it was broken. Figure 44 shows the plastic deformation in the metal below the film after it is broken. Slip bands can be observed on the metal surface. After the surface film broke, the metal appeared to have extensive ductility. We can therefore conclude that grade 2 commercial purity titanium has good plasticity once the film is broken.It should be noted that these results were obtained at an extreme condition, i.e., a very large cathodic hydrogen charging current density.

Both smooth type B specimens and notched specimens were charged at different well-controlled electrochemical potentials as they were pulled in tension. These tests were run in 6%NaCl solution with a pH of 1 at a temperature of 70°C. Mechanical tests were performed in oil at the same temperature to obtain results for an inert environment. Figure 45 shows the ratio of the elongation-to-fracture in solution to the elongation-to-failure in oil for smooth specimens at different applied potentials. The crosshead speed was $7x10^{-3}$ mm/min. There was a slight indication that the hydrogen embrittlement susceptibility increased with decreasing applied potential, but the decrease in elongation in the testing solution was very small. The elongation decreased less than 10% even at a potential

-1400mV_{SCE}. Ductile fracture surfaces were found for all tests, including the inert environment.

Selenium has a high hydrogen overpotential and acts as a cathodic poison. When selenium is plated out at the crack tip, the rate of the hydrogen recombination reaction is reduced, thus promoting hydrogen absorption. Additions of 600 ppm selenium to the test solution produced no further decrease in elongation at cathodic potentials of -1000, -1200 and -1400mV_{SCE}. Therefore, it appears that the smooth specimens for grade 2 titanium are not susceptible to hydrogen embrittlement.

Figure 46 shows the ratio of elongation-to-fracture in NaCl solution to the elongation-to-failure in oil for notched specimens at different applied potentials. The crosshead speed was $7x10^{-3}$ mm/min. There was no significant change in elongation at different applied potentials, but a small decrease was observed compared to the elongation in an inert environment. The fracture mode for notched specimens was ductile at this crosshead speed, even at a cathodic potential of -1400mV_{SCE}. Figure 47 shows the appearance of the fracture surface in oil and at cathodic potentials. At more negative potentials, it is anticipated that the fracture surface, such as that shown in Figure 47c, will be covered by a thin hydride film. Also, in these samples secondary cracks were observed as shown in Figure 47d.

As described earlier in this report Scully (22) indicated that the decrease in elongation for titanium in sea water strongly depended on the equivalent oxygen content in titanium. If we calculate the value of the equivalent oxygen content for this alloy, we find that it it is 0.17%. The results shown in Figure 10 would indicate that the change in elongation when exposed to NaCl should be less than 10%. This prediction agrees with out results.

An additional concern was what effect strain rate could have on the hydrogen embrittlement of titanium. Figure 48 shows the variation of hydrogen embrittlement susceptibility for titanium with the crosshead speed at an applied potential of -1400mV_{SCE}. At a crosshead speed, $7x10^{-2}$ mm/min, there was practically no decrease in the elongation in the solution. At a crosshead speed of $7x10^{-3}$ mm/min, some decrease in elongation was observed. However, at $7x10^{-4}$ mm/min, the elongation did not change further compared to that observed at $7x10^{-3}$ mm/min. Figure 49 shows the variation of the thickness of the hydride film with the crosshead speed at an applied potential of -1400 mV_{SCE}. The thickness of the hydride film increased with decreasing crosshead speed. Based on the results shown in Figures 40 and 42, the elongation should decrease with increasing thickness of the hydride film on the surface; however, it was not the case for the notched specimens. For the notched specimen, the HE susceptibility was not dependent on the

thickness of the hydride film for the unstrained surface, but was dependent on the thickness of the hydride film at the crack tip. Figure 50 shows the cross section of the specimen along the loading direction after necking of the specimen at two different crosshead speeds. It was found that the thickness of hydride film for the unstrained surface was different at two different speeds, but the difference in thickness of the hydride film at the crack tip was small. Due to the crack growth from the notch of the specimen and low diffusion rate of hydrogen in titanium, the hydride film at the crack tip had not become very thick, and this would not have a great effect on the mechanical properties.

Previous investigations of grade 2 titanium in synthetic sea water showed no loss of ductility as a function of the cathodic potential, and no clear trend in the measured parameters was noticed (38). This behavior should be associated with low penetrability and solubility of hydrogen in grade 2 titanium. Hydrogen adsorption in titanium has traditionally been considered to be a problem only at temperatures above 80 °C, where the diffusion rate of the hydrogen becomes significant. Jacobs and McMaster (36) have published a curve which indicates that no appreciable diffusion of the hydrogen in alpha titanium occurs at temperatures below 80 °C. This was also supported by the work of Phillips *et al.* (13) in which they measured the diffusion coefficient in titanium over the temperature range from 25 to 100 °C; for example, the diffusion rate of hydrogen in alpha titanium was about $1x10^{-11}$ cm^2/s at 40 °C and $3.2x10^{-12}$ cm^2/s at 25 °C. A low diffusion rate of hydrogen will result in difficulty in hydrogen absorption and in the ability to form a hydride film at a growing crack tip.

The low solubility of hydrogen in grade 2 titanium is another reason responsible for low HE susceptibility to titanium. The solubility of hydrogen in titanium varies with temperature, pressure, chemical purity, alloy composition, stress and deformation. Room temperature solubility of hydrogen is typically cited as ranging from 20 to 200 ppm and is lower in alloys containing oxygen (39-41). It was observed that high purity titanium would not absorb measurable amounts of hydrogen after electrolytic charging, while substantial hydrogen absorption was detected in commercial purity grade 2 titanium. Work by Pound (42) indicated that, in the case of Ti grade 2 compared to pure titanium, interstitial nitrogen appears to be the principal irreversible trap at low hydrogen levels, although grain boundaries are another possibility. When the concentration of hydrogen becomes high enough, hydride formation provides an additional form of trapping. Alloying, particularly with molybdenum, also increases hydrogen solubility. Charlot (43) studied hydrogen absorption of commercially pure titanium and titanium with 2% Ni and indicated that commercially pure titanium was immune to hydrogen pick-up except when coupled to aluminum; however, the Ti-2Ni alloy absorbed considerable hydrogen when

coupled with nickel, copper, stainless steel or as an uncoupled control. Sensitivity to the hydrogen assisted stress cracking has been more evident for Ti grade 12 (21,38). It suffered some loss of ductility, mainly manifested in the reduction of area and consequently in the true stress at fracture. In case of grade 12, the small amount of β-phase, which has a much higher diffusion coefficient for hydrogen than the α-phase (44), helps the hydrogen penetrate into the material. However, when saturation of hydrogen is reached, hydrides precipitate in the α-phase along the grain boundaries.

5.0 CONCLUSIONS

1. The corrosion potential and cathodic reaction rate increased with decreasing pH value and increasing temperature. Both the decrease of pH value and the increase of temperature increased the cathodic reaction process more strongly than anodic reaction process.
2. The corrosion potential changed when titanium was coupled with other metals. Naval brass and monel always anodically polarized titanium; zinc and aluminum cathodically polarized titanium. HY80 can both anodically and cathodically polarize titanium, depending on temperature. Above 50°C, titanium is the cathode.
3. Hydrides formed when the electrochemical potential decreased below -600 mV_{SCE}. When naval brass, monel and inconel were coupled with titanium, the potential was above this value and no hydrides could be detected on the surface. Hydrides could be found on the titanium surface when titanium was coupled with HY80 in solution at 70°C and 90°C. Hydrides were detected when titanium was coupled with aluminum and zinc in solution at all temperatures.
4. Plate-shaped hydrides formed on the titanium surface when titanium was cathodically charged. Its thickness varied with testing conditions, including temperature, pH value, applied potential or current density and hydrogen charging time. All hydrides were found to form near the surface; no hydrides were found in the interior of the material.
5. Although hydrides could be found on the titanium surface during cathodic hydrogen charging, they had little effect on the mechanical properties of the material. Mechanical tests for smooth and notched specimens showed little decrease in elongation under prior or dynamic hydrogen charging, even at very slow crosshead speeds.
6. Hydride films at the crack tip could not become very thick due to crack growth and the low diffusion rate of hydrogen. On the other hand, after the hydride film was broken, it did not affect mechanical properties.

The low hydrogen diffusion rate and the high purity of titanium were responsible for its low hydrogen embrittlement susceptibility.

6. PLANNED WORK FOR THE COMING YEAR

The following tasks will be undertaken during the second year of this work. This work will investigate in detail the mechanisms of hydrogen embrittlement in these materials.

(1.) The first task will be to characterize in detail the formation of the hydride. This work will involve both analytical characterization of the hydride and its formation (for example, with repect to the Ti lattice and the temperatures at which it dissolves and precipitates) and a detailed analysis of its effects on the mechanical and corrosion properties of the titanium. This latter work will involve careful fractographic analysis of these tests, including the crystallographic determination of the crack path.

(2.) The second task will be to perform permeation tests to determine the rate of hydrogen absorption and the diffusivity of hydrogen in grade 2 titanium. These tests will be run by setting up an electrochemical cell and allowing hydrogen to enter the metal on one side. The emission of hydrogen on the opposite side of the sample will be detected electrochemically. In that way we can determine the time required for hydrogen to permeate a given distance. We will also measure the progression of the hydride layer through the sample by optical metallography.

(3.) In all of the above tests, the grade 2 titanium will have an equiaxed structure. For the third task, we will select a set of specfic conditions and compare the results on titanium samples with different microstructures. The analysis tehcniques described in phase I will also be used here.

(4.) Since Scully (22) predicted oxygen should have a significant effect on susceptibility to hydrogen embrittlement of these materials, we will obtain some grade 3 titanium which contains higher oxygen concentrations and run mechanical tests in which the titanium is dynamically charged. These results will be compared with those obtained on grade 2 titanium.

7. REFERENCES

1. Titanium Offshore - A Designers and Users Handbook, The Titanium Information Group, January 1996

2. The Corrosion Resistance of Titanium, TIMET Bulletin, 1996

3. Solving Some Seawater Corrosion Problems with Titanium, G. Baker and J.S. Grauman, Sea Technology, April, 1991.

4. The Use of Titanium to Eliminate Corrosion Concerns in Service Water Piping Systems - A Corrosion Immunity and Economic Analysis, TIMET Presentation to EPRI, April, 1992.

5. Codeweld Ti Tubing, TIMET Bulletin, March 1996.

6. Subsea Manned Engineering, GFK Haux, Best Publishing Co., 1982.

7. Corrosion Resistance of Titanium, Imperial Metal Industries, Ltd., Birmingham Technical Report

8. K. Shimogori, H. Sato, F. Kamikubo, and T. Fukuzuku, Desalination, **22**, 403 (1977).

9. L.C. Covington, Corrosion, **35**, 378 (1979).

10. R. W. Schutz and J.S. Grauman, Corrosion 89, Paper 110, April 17-21, 1989, New Orleans.

11. T. Fukuzuku, K. Shimogori, H. Satoh, F. Kamikabo, Desalination,

12. H. Sato, T. Fukuzuka, K. Shimogori, and H. Tanabe, Second International Conference on Hydrogen in Metals, Paper 6A1, Paris, 1977.

13. I.I. Phillips, P. Poole, and L.L. Shreir, Corrosion Science, **14**, 533 (1974).

14. J.B. Cotton, Chem. Engr. Progress, **66**, 57, (October, 1970).

15. H. Numakura, K.Koiwa, H. Asano, H. Murata, and F. Izumi, Scripta Metall., **20**, 213 (1986).

16. O.T. Woo and G.J.C. Carpenter, Scripta Metall. **19**, 931 (1985).

17. G.S. Lenning, C.M. Craighead, and R.I. Jaffee, Trans. AIME, 367 (1954).

18. A. Efron, Y. Lifshitz, I. Lewkowicz, and M.H. Mintz, Journal of the Less Common Metals, **153**, 23 (1989).

19. J. Liu and K. Nakasa, Trans. Japan Inst. Metals, 1261 (1990).

20. S. Sato, K. Nagata, Y. Watanabe, T. Nakamura, and T. Hamada, Corrosion Eng. Japan, **25**, 311 (1976).

21. H. Jain, T.M. Ahn, and P. Soo, Corrosion, **41**, 375 (1985).

22. D.J. Simbi and J.C. Scully, Corrosion Sci., **37**, 1325 (1995).

23. J.R.B. Gilbert, Proc. Conf. Titanium Science and Tech., **2**, 1105 (1984).

24. David Litvin and David E. Smith, Naval Engrs. Journal, Oct. 1971, p. 37

25. F. Sedillot, C.G. Doris, and A. Stevenson, Offshore Technology Conference, 1982, p. 341.

26. D. Livingston, Ocean Industry, p. 65 (July, 1979).

27. J.D. Boyd, ASM Trans., **62**, 977 (1969).

28. J.A.S. Green, B.W. Gamson, and W.F. Westerbaan, Desalination, **22**, 359, (1977).

29. E.G. Bohlmon and F.A. Posey, Proc. First Internat. Conf. on Water Desalination, Washington, D.C., p. 306 (1965).

30. G.A. Moudry, Water and Water Eng., p. F-17 (November, 1969).

31. S. Kido and T. Shinohara, Desalination, **22**, 369, (1977).

32. Annual Book of ASTM Standard, Part 31, D1141, p.48 (1976).

33. A.J. Sedriks, Materials Performance, Feb. 1994, p. 56.

34. G. Venkataraman and A.D. Goolsby, Corrosion/96, NACE, Paper 554.

35. T. Nosetani, Sumitomo Light Metal Technical Reports, July, 1974.

36. R.L. Jacobs, J.A. McMaster, Materials Protection and Perf., **11**, 33 (1972).

37. M.L. Wasz, F.R. Brotzen, R.B. McClellan, and A.J. Griffin, Jr., Inter. Mater. Reviews, **41**, 1 (1996).

38. I. Azkarate and A. Pelayo, INASMET, 20009-San Sebastion.

39. A. Jostsons and A.E. Jenkins, Trans. AIME, **239**, 1318 (1967).

40. S. Yamanaka, T. Tanaka, S.Tsuboi, M. Miyake, Fusion Eng. **10**, 303 (1989).

41. T. H. Qyach-Kamimura, D. David, G. Beranger, A. Falanga, G. Lozes, J. Less-Common Metals, **125**, 59 (1986).

42. B.G. Pound, Corrosion, **47**, 99 (1991).

43. L.A. Charlot, US Department of Interior Research and Development Progress Report No. 624, December 1970.

44. W.R. Holman, Trans. AIME, **233** (1965).

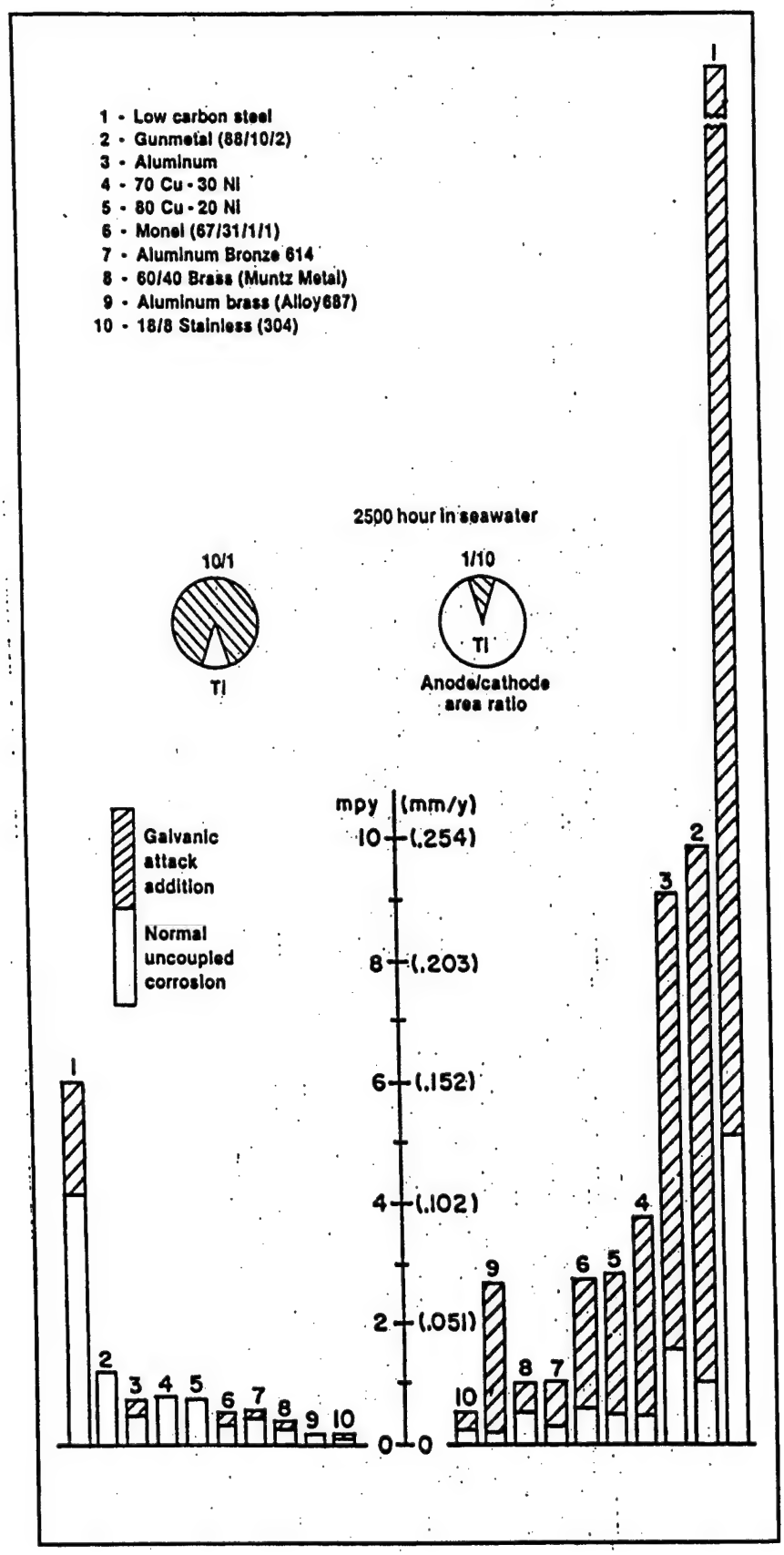

Figure 1 - The corrosion of various metals galvanically coupled with titanium. The left set of data are those obtained when the area ratio of the metal to titanium was 10:1. The right set of data were those obtained when the same area ratio was 1:10. Data taken from reference 2.

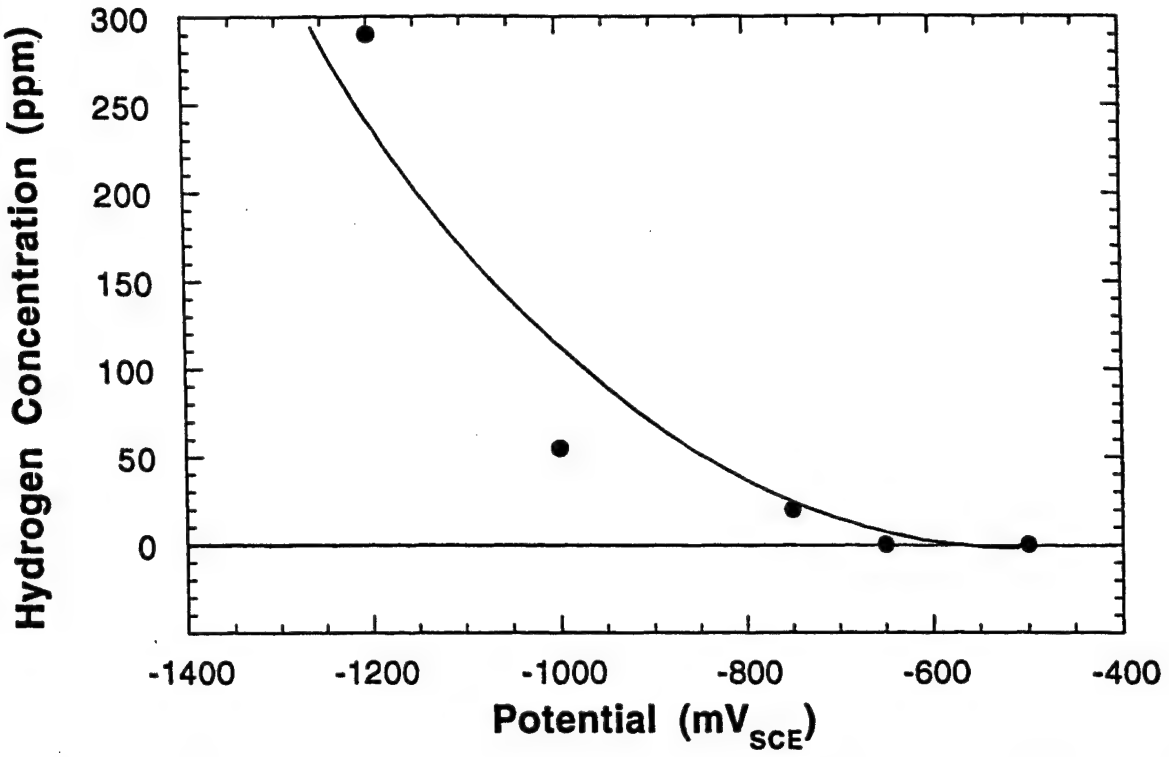

Figure 2 - The concentration of hydrogen in ppm plotted as a function of the electrochemical potential. The testing conditions were: deaerated 6%NaCl, pH=6, 100°C, for a time of 1440 hours. Data taken from reference 8.

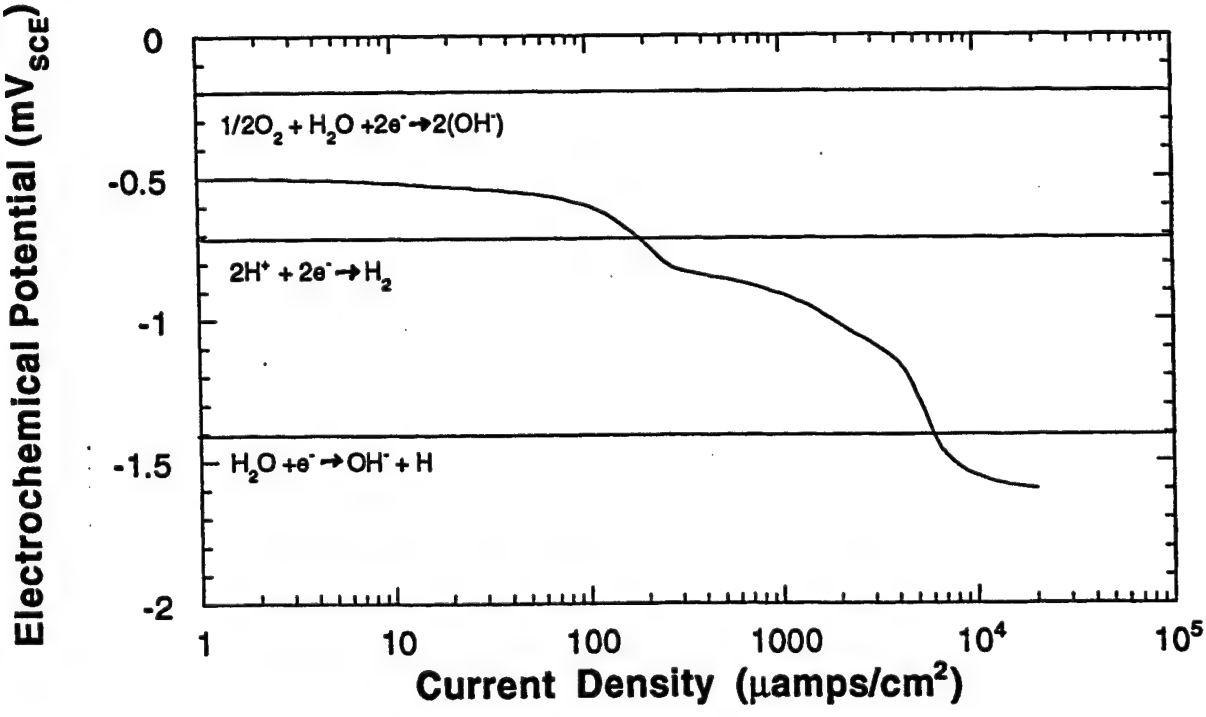

Figure 3 - Cathodic polarization curve for titanium in sea water. (Reference 9)

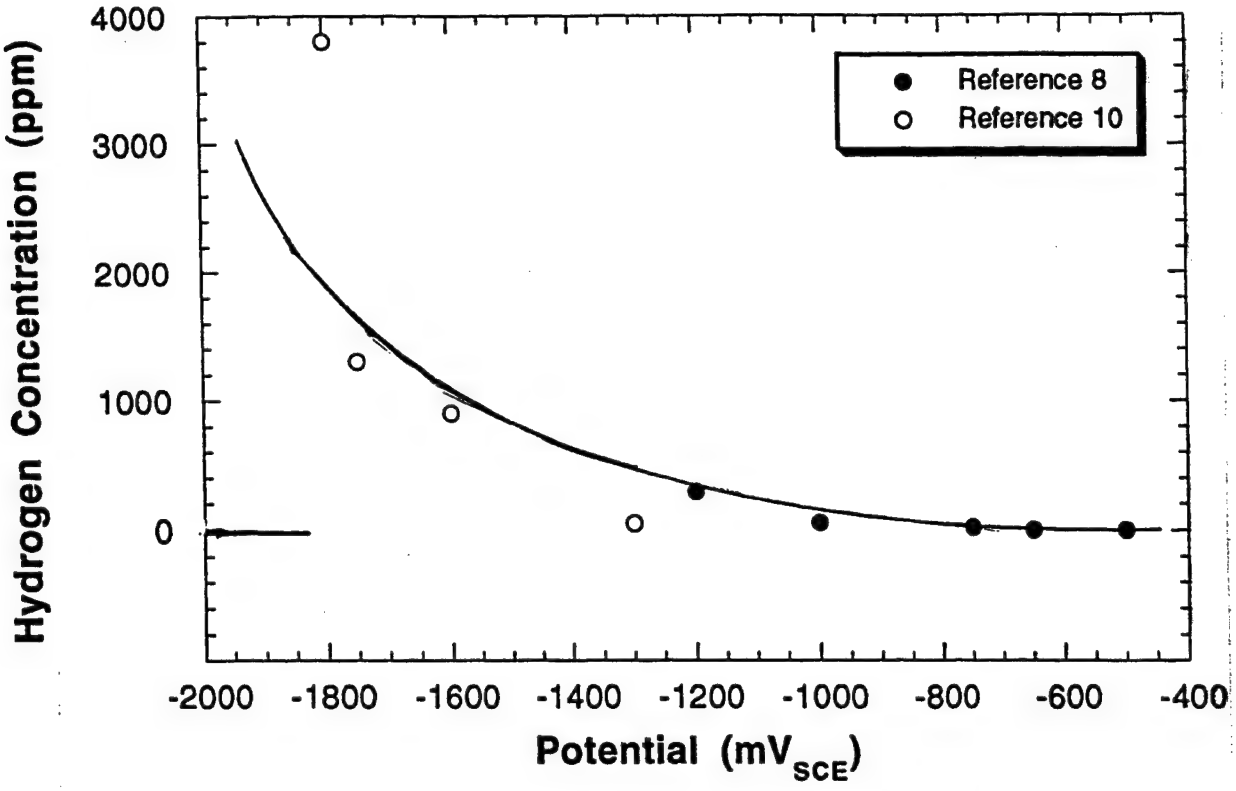

Figure 4 - The hydrogen concentration in ppm plotted as a function of electrochemical potential. The conditions for the data from reference 8 were deaerated 6%NaCl, pH=6, 100°C for a time of 1440 hours. The conditions for the data reported in reference 10 were 3%NaCl, pH=6-9, 45°C for 2160 hours.

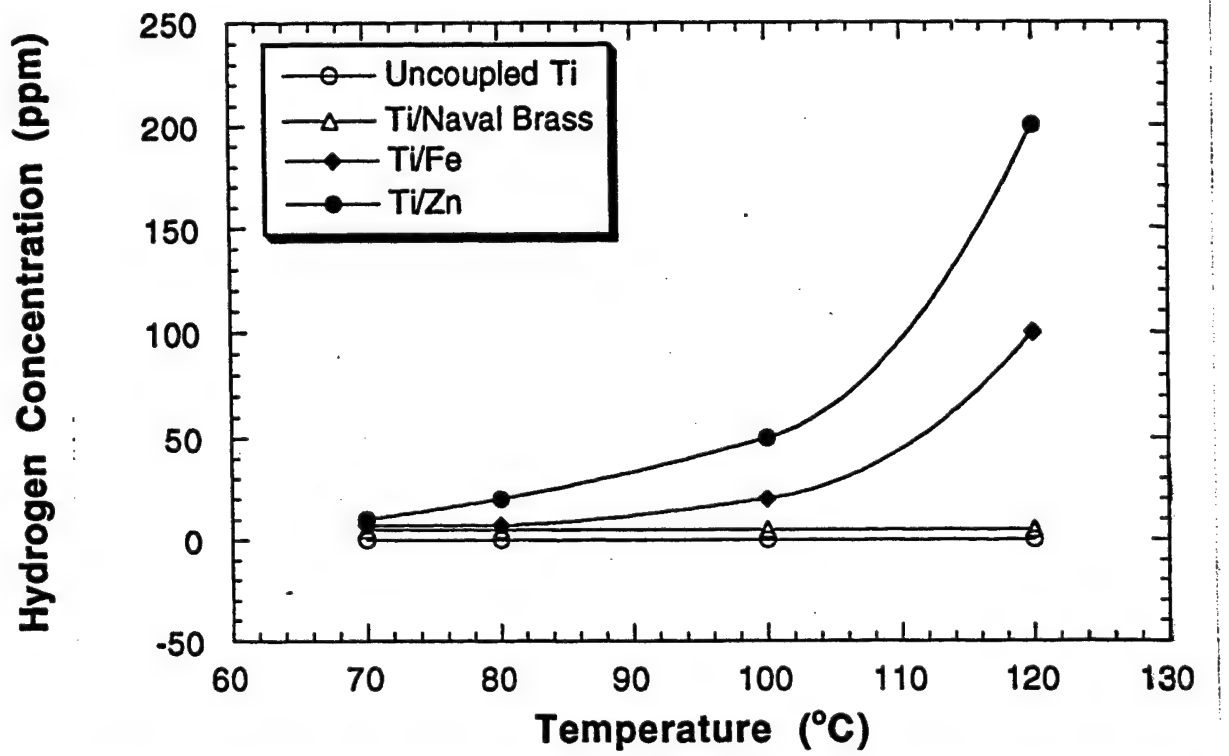

Figure 5 - The effect of galvanic coupling on the hydrogen concentration. The hydrogen concentration in atomic ppm is plotted as a function of temperature for uncoupled titanium and Ti coupled to naval brass, Fe and Zn. The solution was 6%NaCl, pH=6, time=270 hours. Data taken from reference 8.

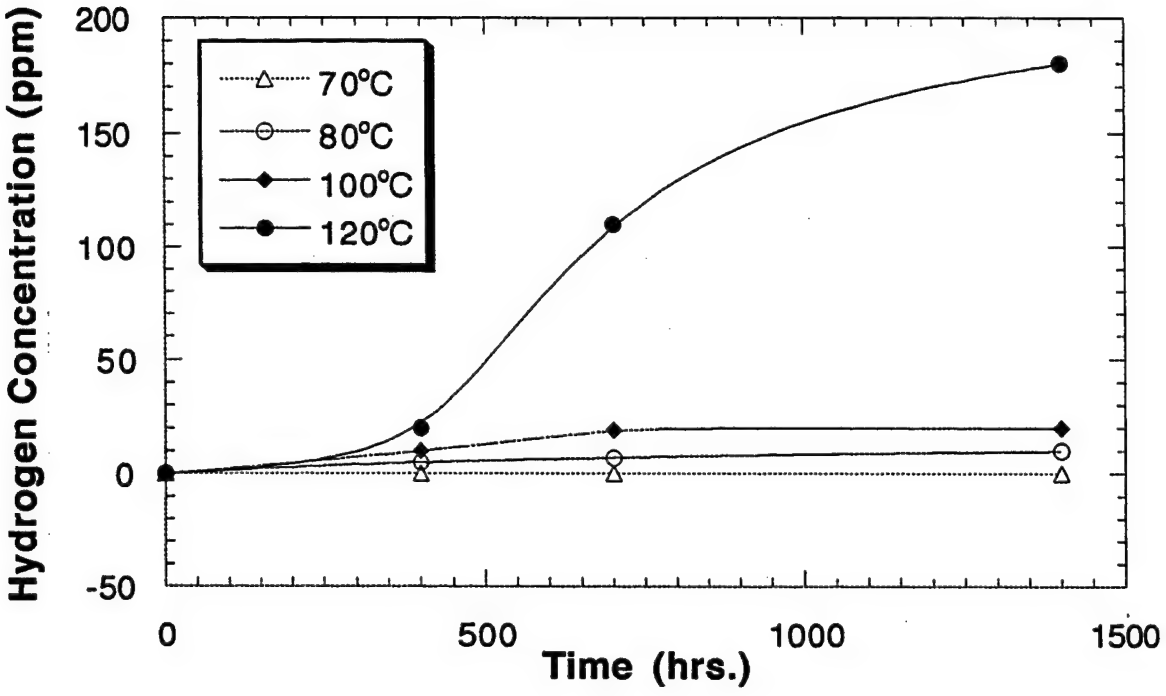

Figure 6 - The hydrogen concentration plotted as a function of time for samples of commercial purity titanium galvanically coupled with steel. Results are given for four different temperatures. The solution was 6%NaCl and the pH was 6. Data taken from reference 8.

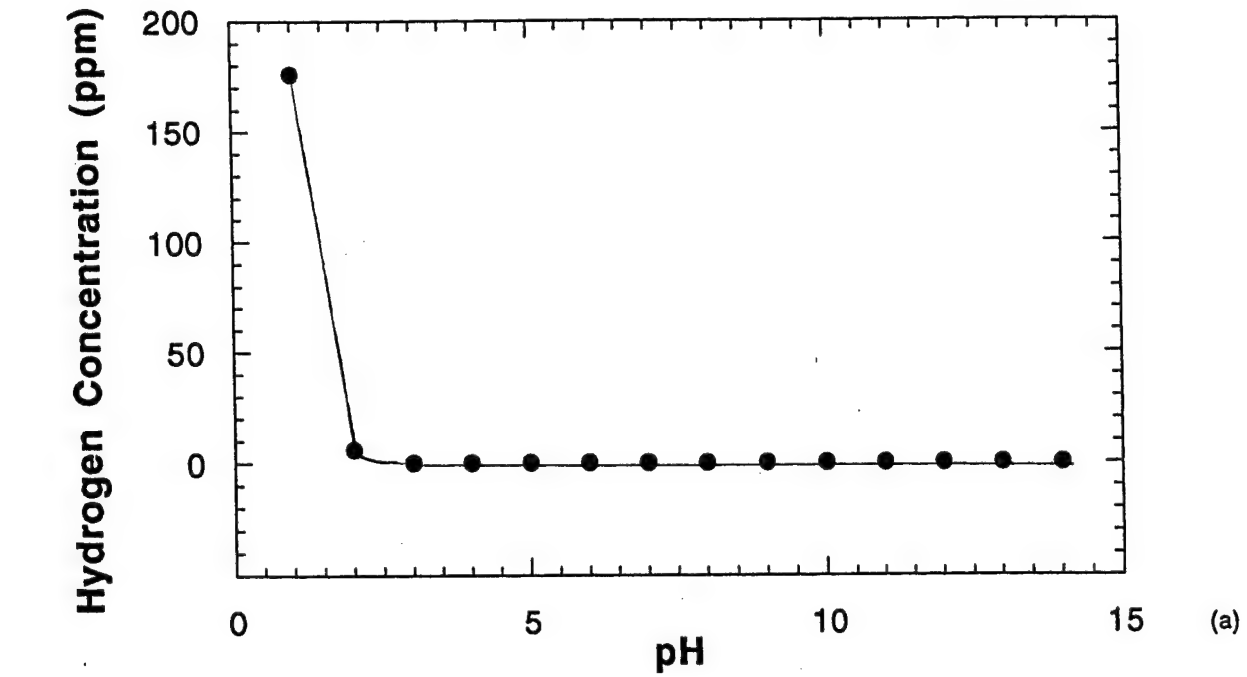

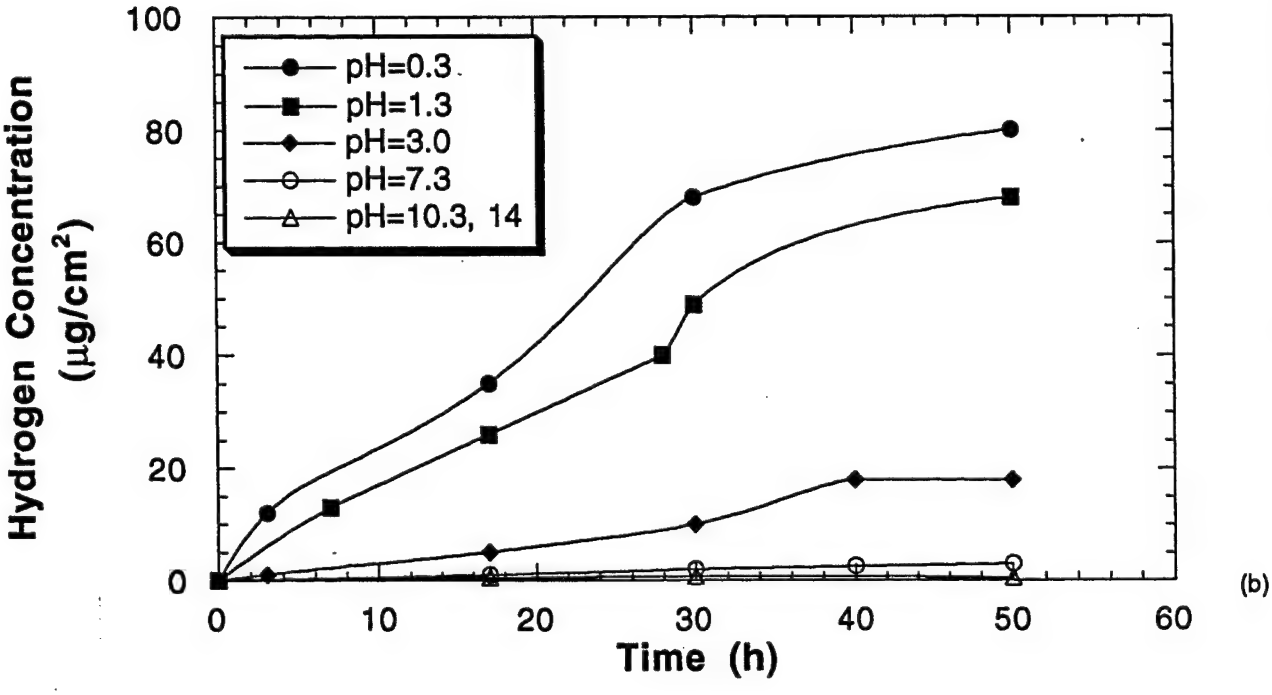

Figure 7 - The effect of pH on hydrogen pick-up. (a) The hydrogen concentration plotted as a function of pH. The solution was 3.5%NaCl, T=90°C, current density 9 mA/cm^2, and electrochemical potential -1900 mV_{SCE}. (b) Hydrogen concentration plotted as a function of time for different pH values. The solutions were varied to give the different pH values. These results were obtained at room temperature at a current density of 0.3 mA/cm^2.

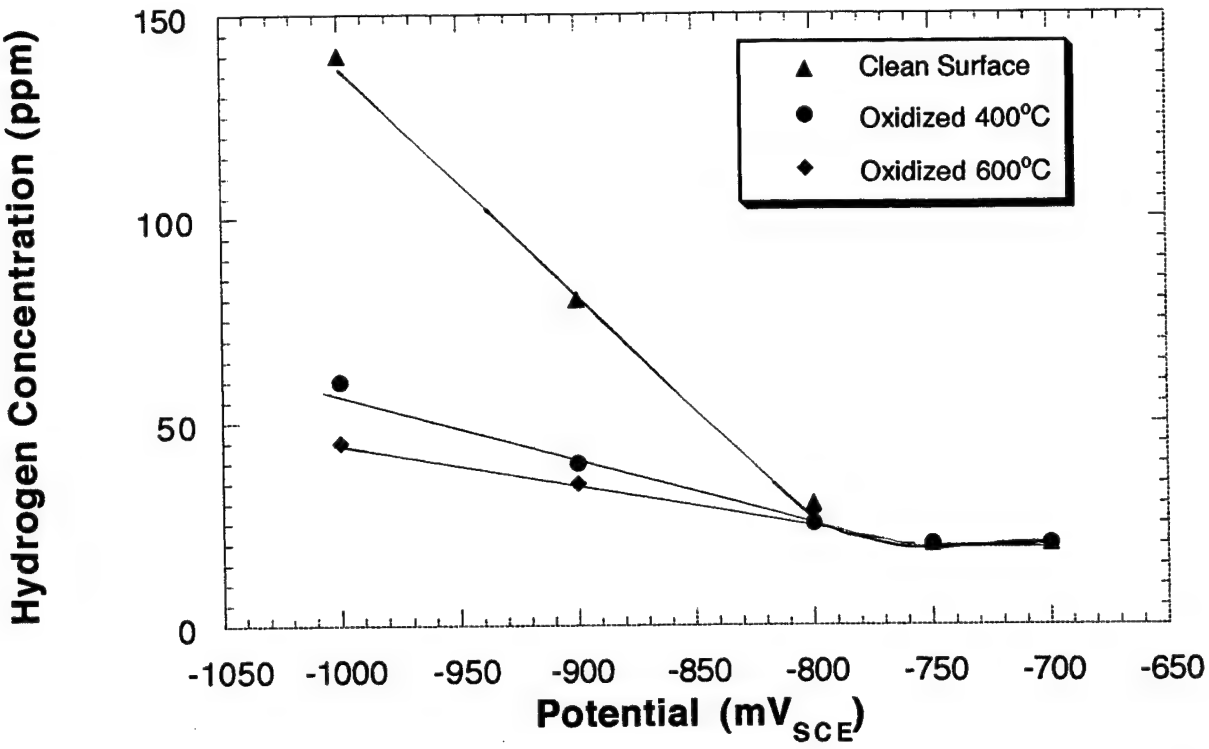

Figure 8 - Hydrogen concentration plotted as a function of applied potential for samples given different pre-treatments. One set of samples has a clean surface. The others had been oxidized at different temperatures. Data taken from reference 12.

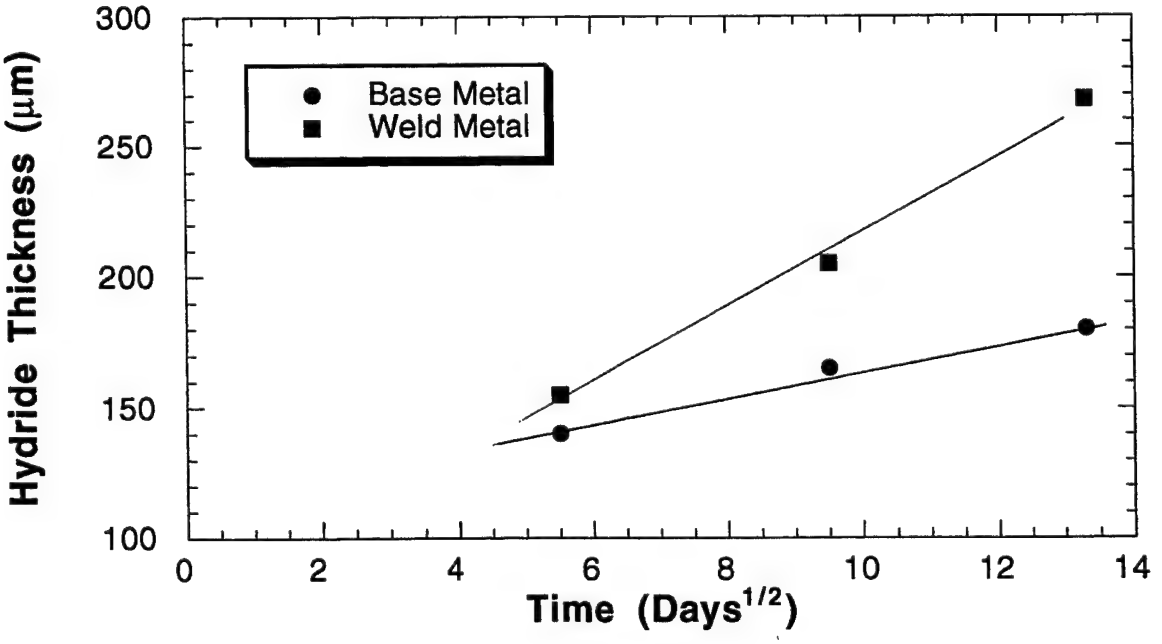

Figure 9 - The average thickness of the hydride layer plotted as a function of time for samples held at an electrochemical potential of -1600 mV_{SCE} at 45°C. Data taken from reference 10.

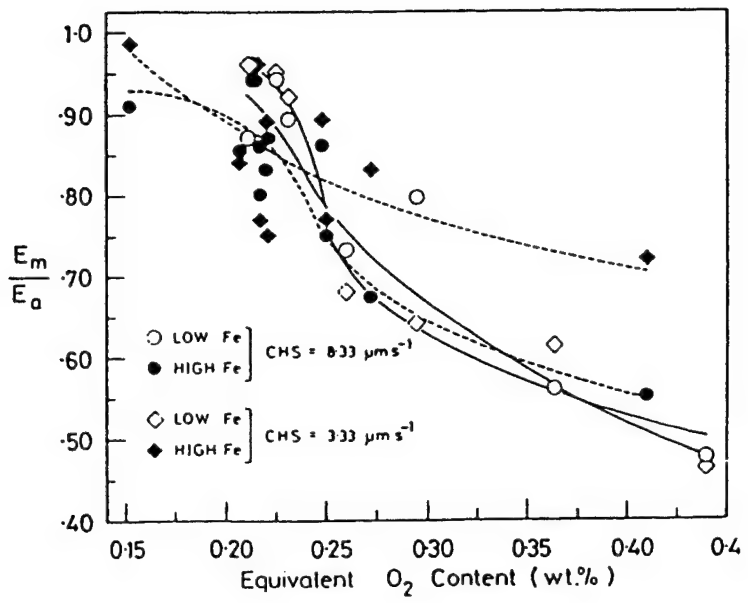

Figure 10 - The elongation to failure plotted as a function of the oxygen equivalent concentration for titanium. Data taken from reference 22.

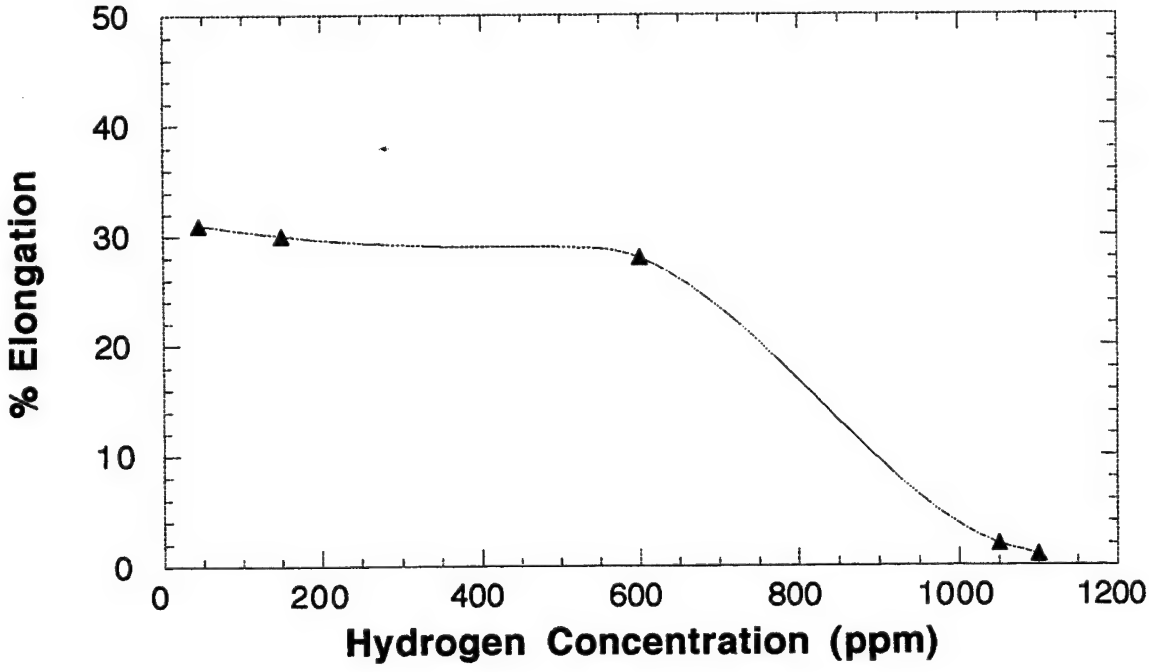

Figure 11 - The elongation to failure plotted as a function of hydrogen concentration in titanium. Data taken from reference 20.

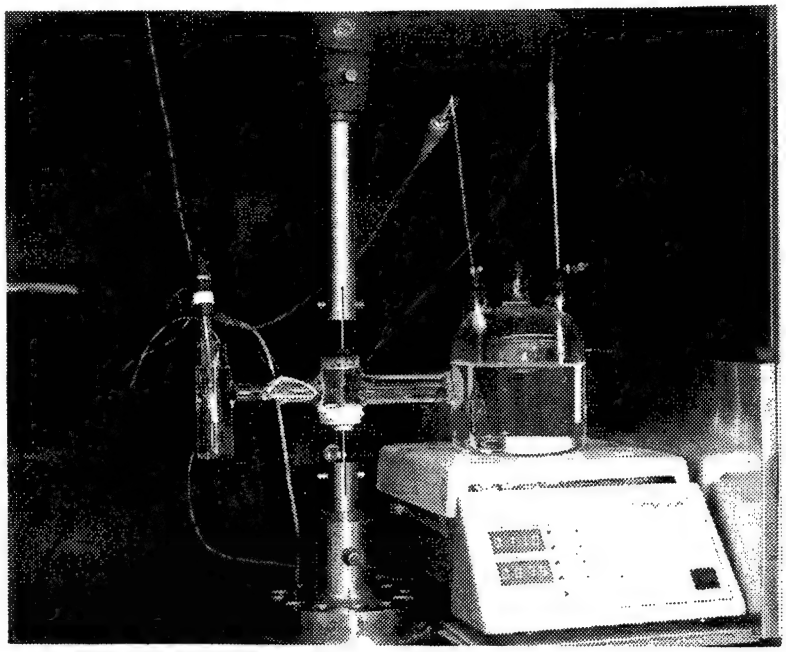

Figure 12 - Setup for the mechanical test.

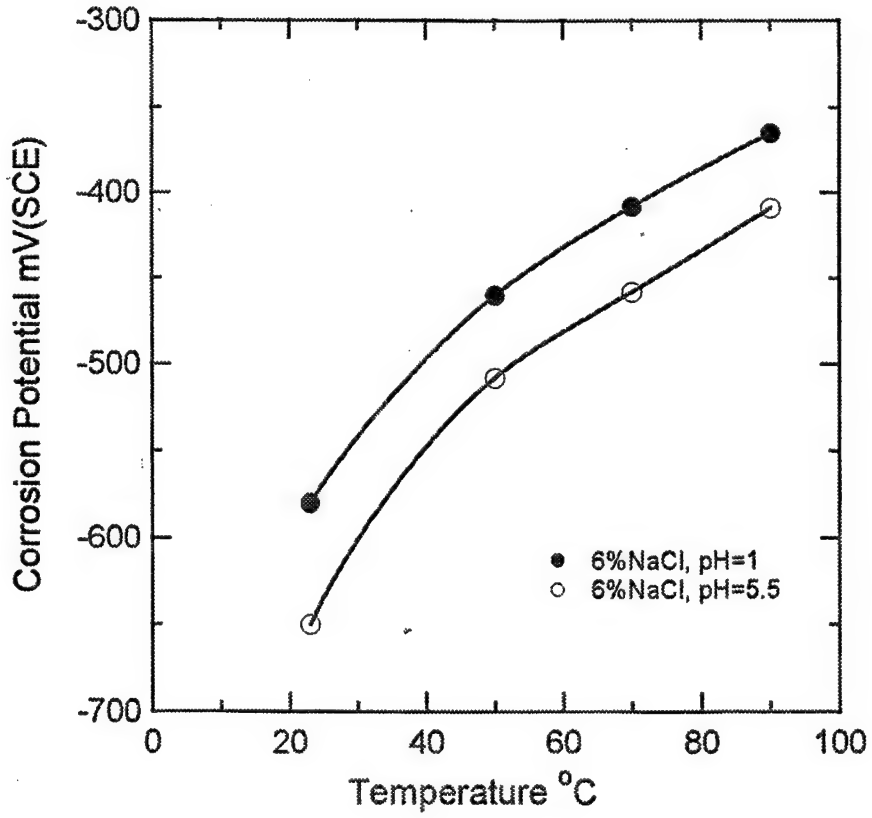

Figure 13 - The variation of the corrosion potential with temperature for titanium in 6%NaCl solution.

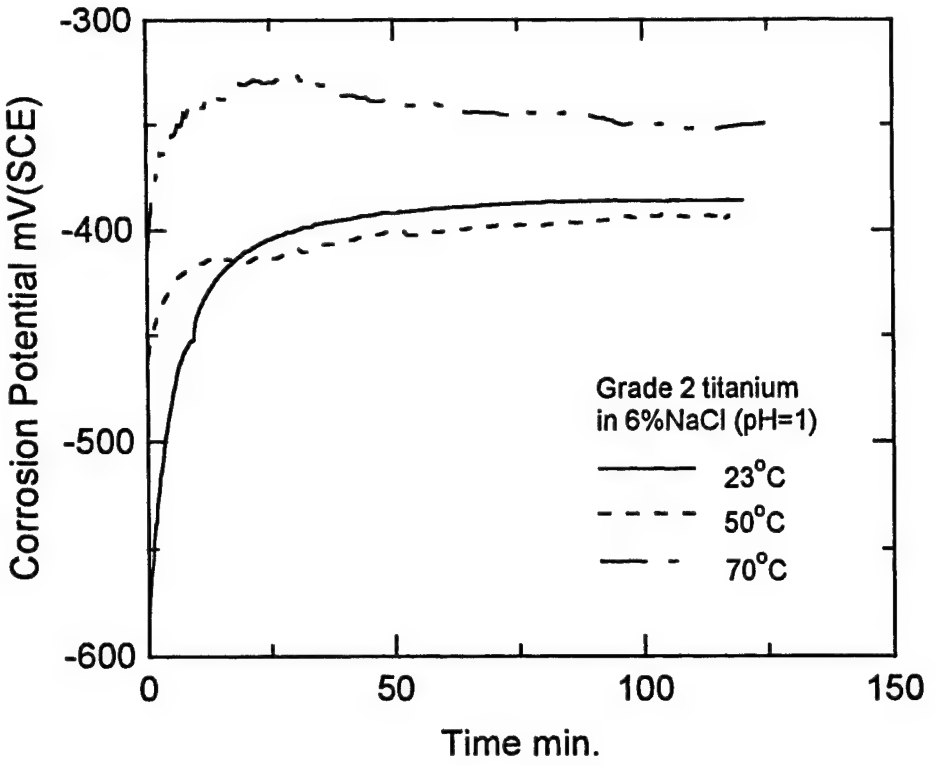

Figure 14 - The variation of the corrosion potential with time for titanium in 6%NaCl solution with a pH=1.

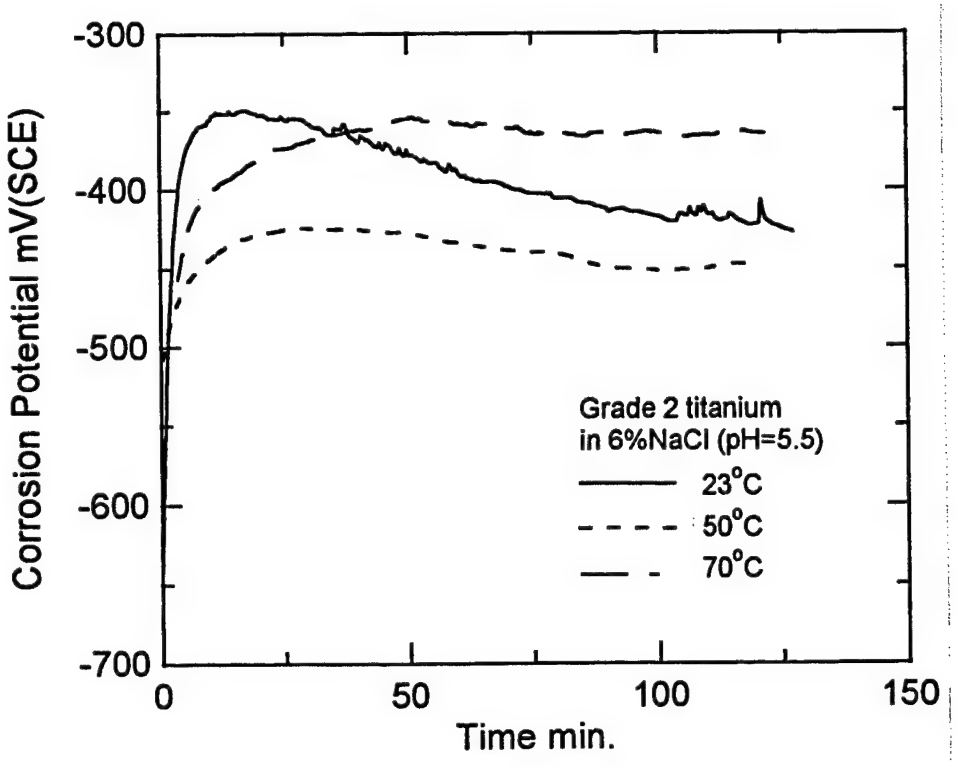

Figure 15 - The variation of corrosion potential with time for titanium in 6%NaCl solution with a pH=5.5.

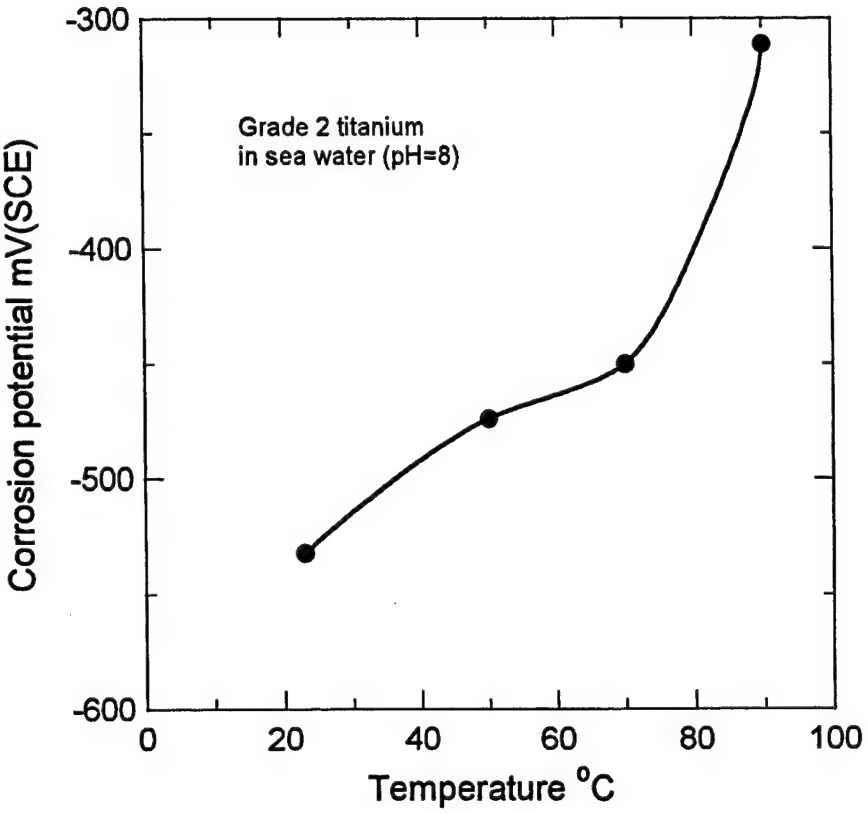

Figure 16 - The variation of the corrosion potential with temperature for titanium in sea water.

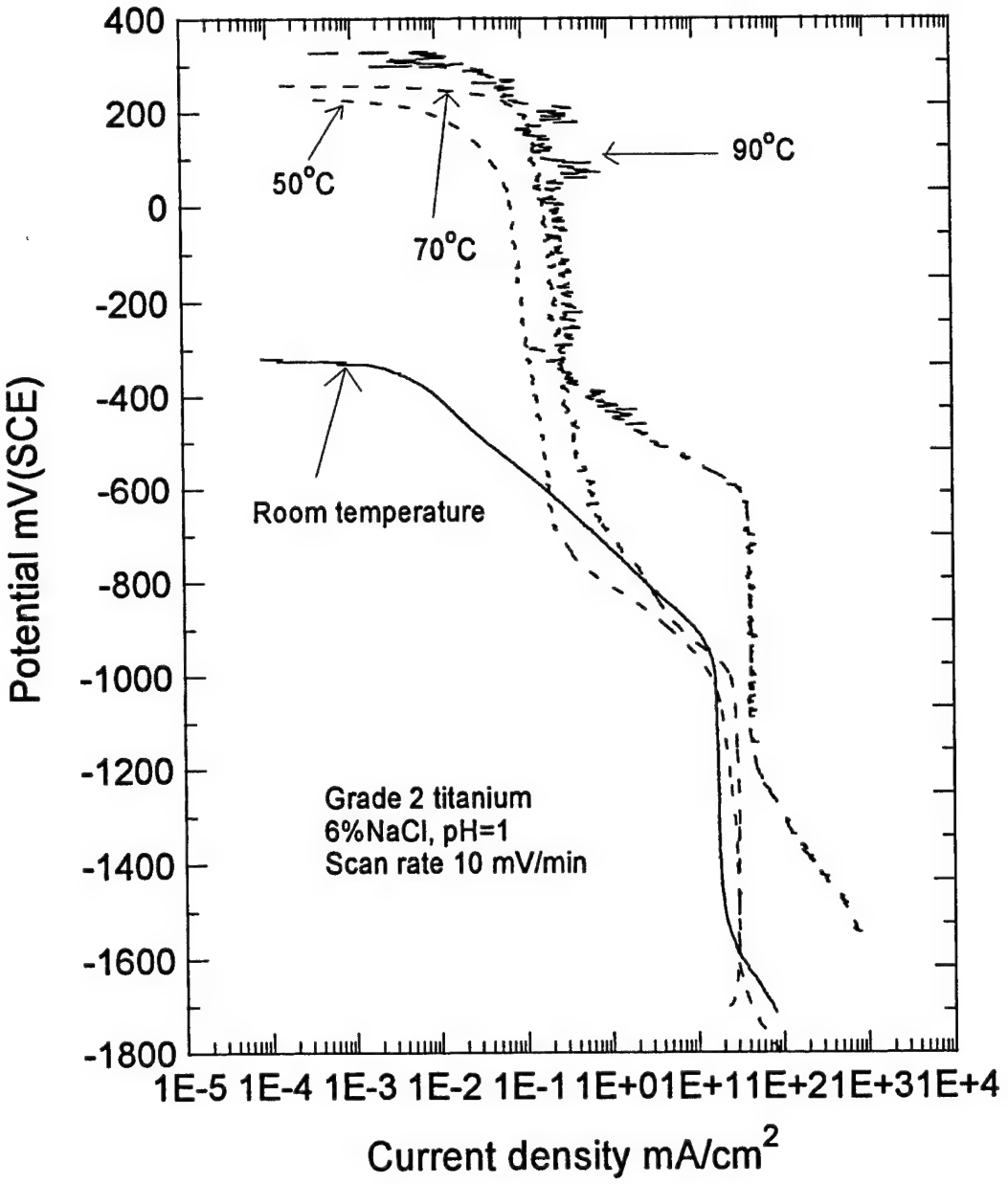

Figure 17 - Cathodic polarization curves at various temperatures for titanium in 6%NaCl solution with a pH=1.

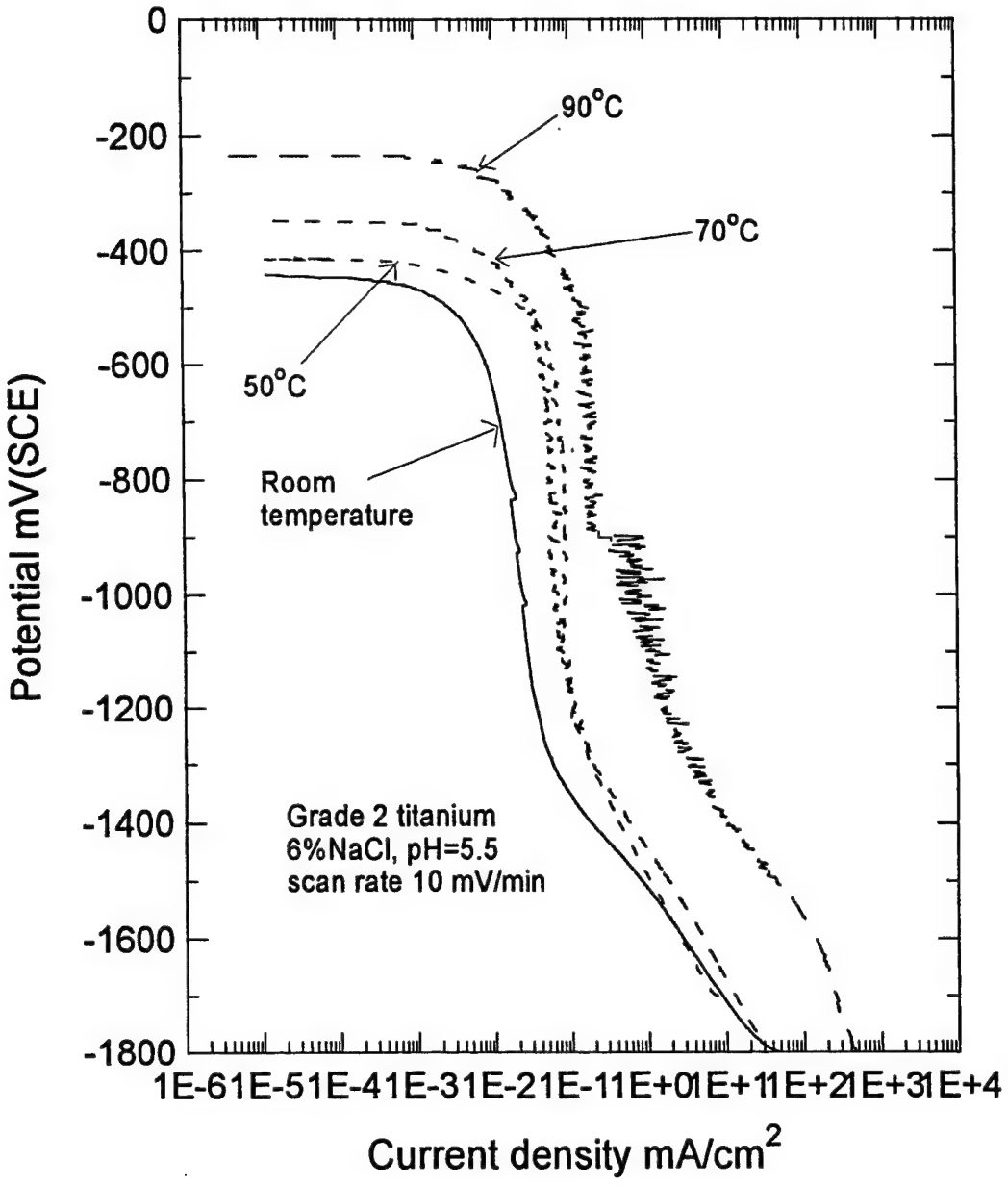

Figure 18 - Cathodic polarization curves at various temperatures for titanium in 6%NaCl solution with a pH=5.5.

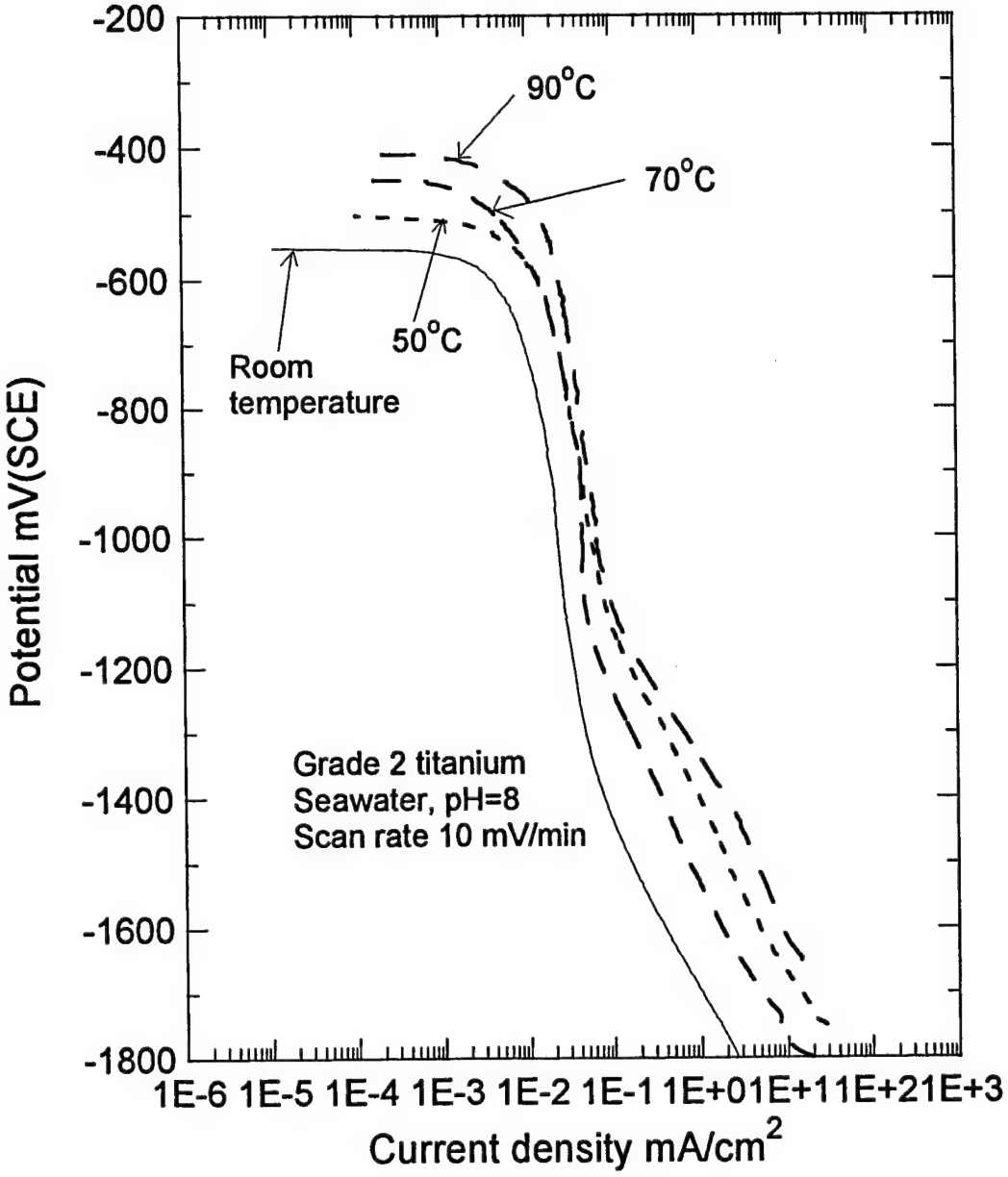

Figure 19 - Cathodic polarization curves at various temperatures for titanium in sea water

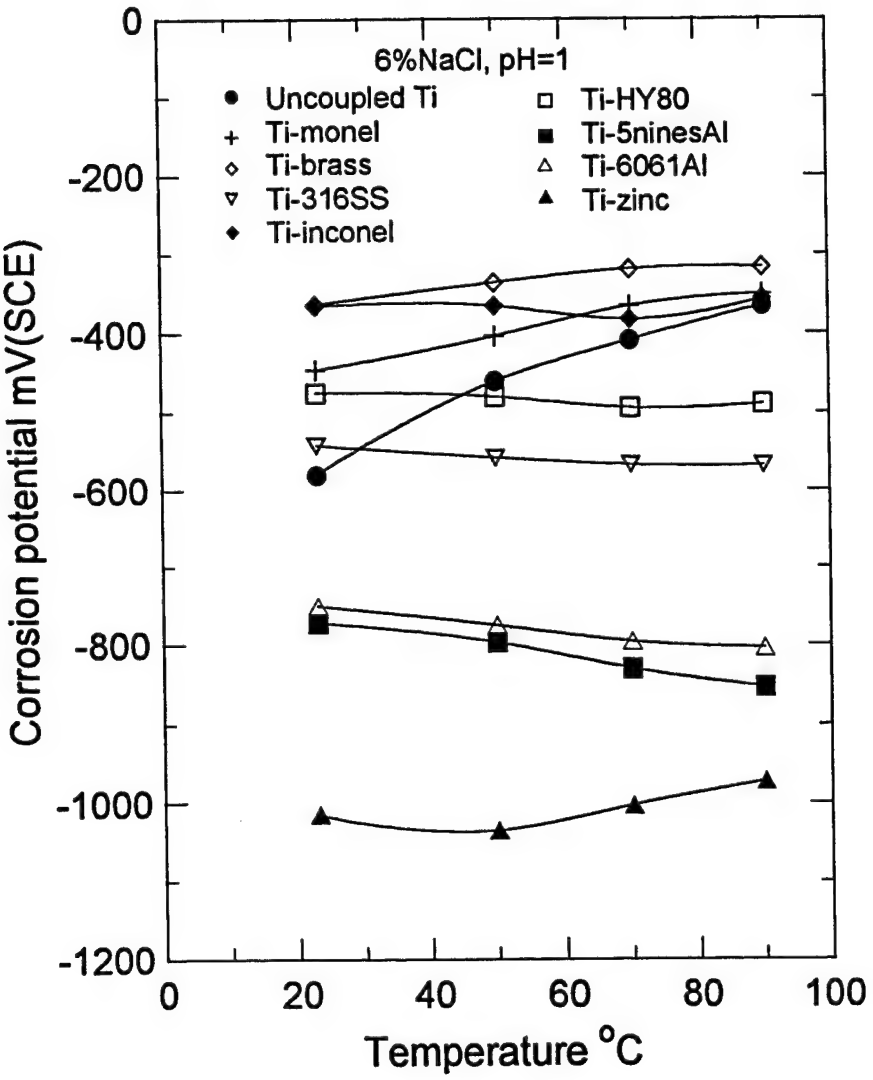

Figure 20 - The corrosion potential plotted as a function of temperature for titanium coupled with different metals in 6%NaCl solution with a pH=1.

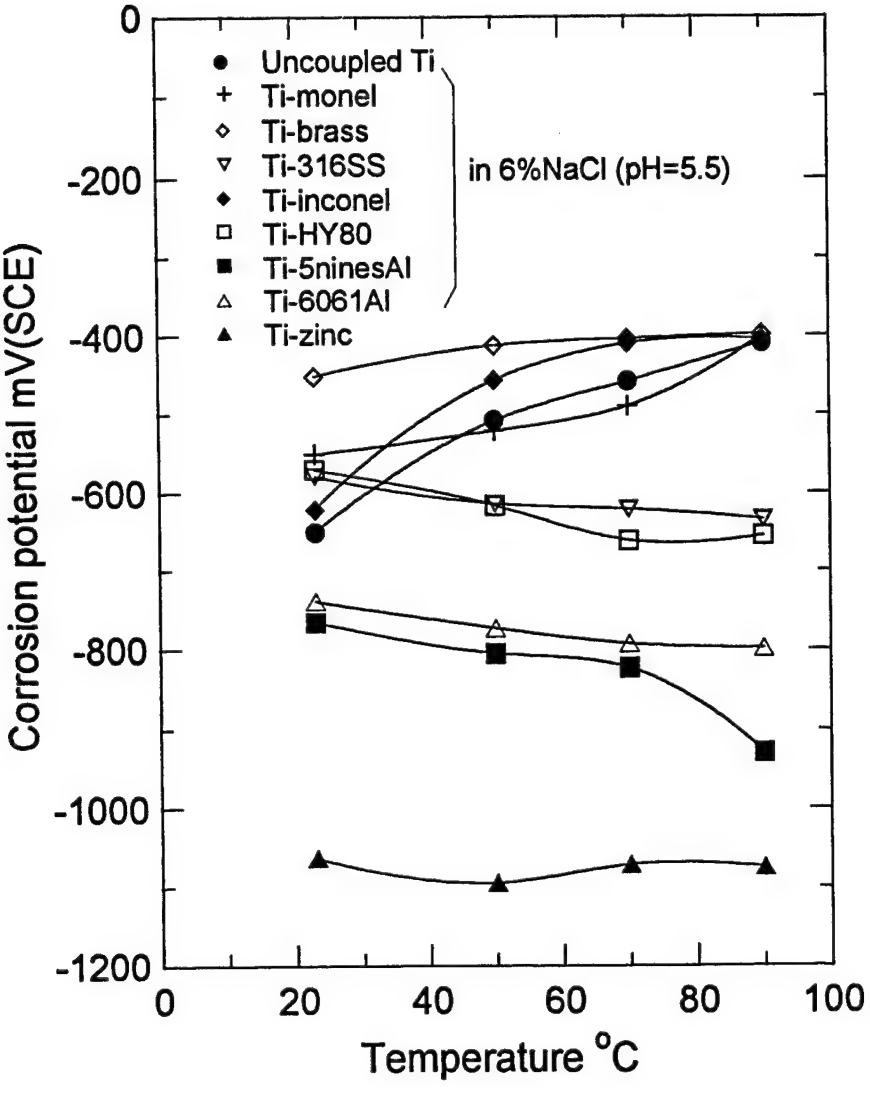

Figure 21 - Corrosion potential plotted as a function of temperature for titanium coupled with different metals in 6%NaCl solution with a pH=5.5.

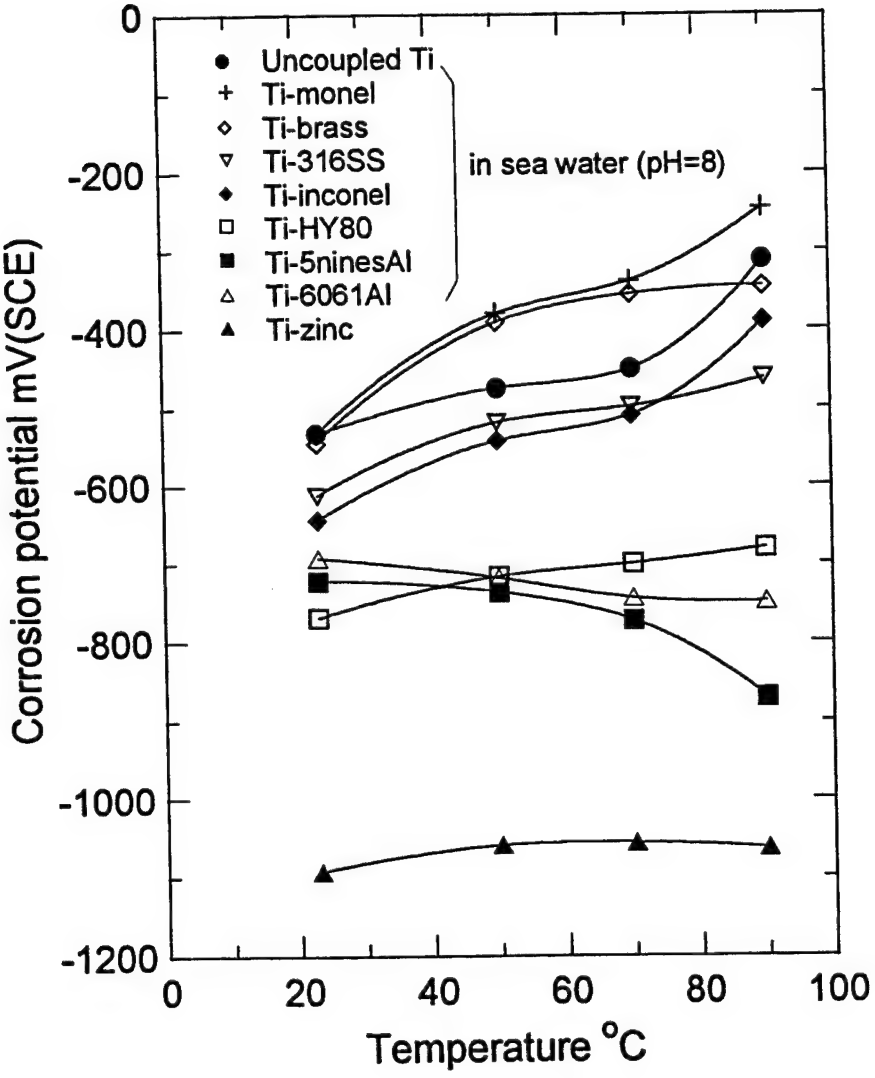

Figure 22 - Corrosion potential plotted as a function of temperature for titanium coupled with different metals in sea water.

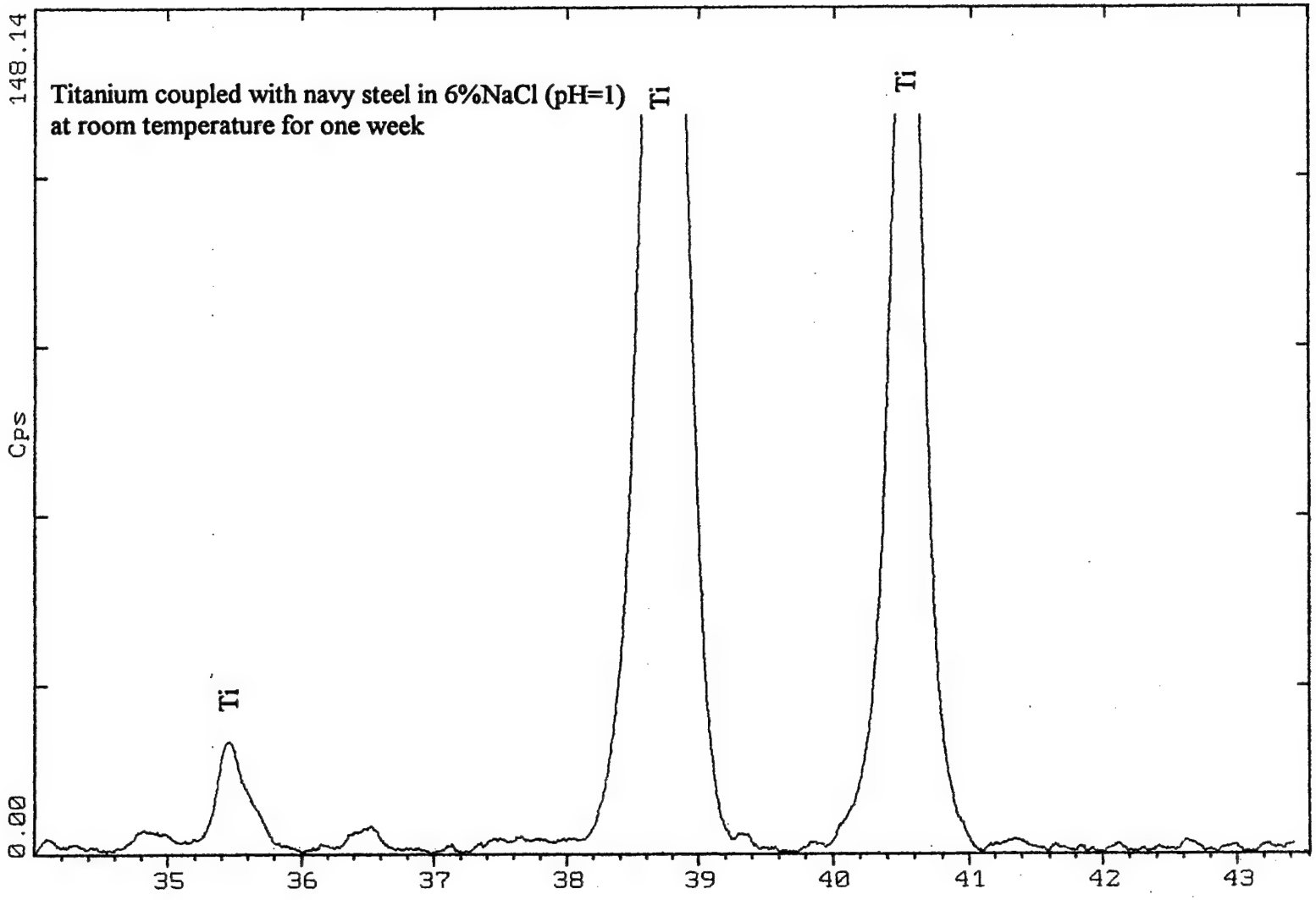

Figure 23 - XRD pattern obtained from titanium coupled HY80 sample after being exposed in 6%NaCl solution (pH=1) at room temperature for one week.

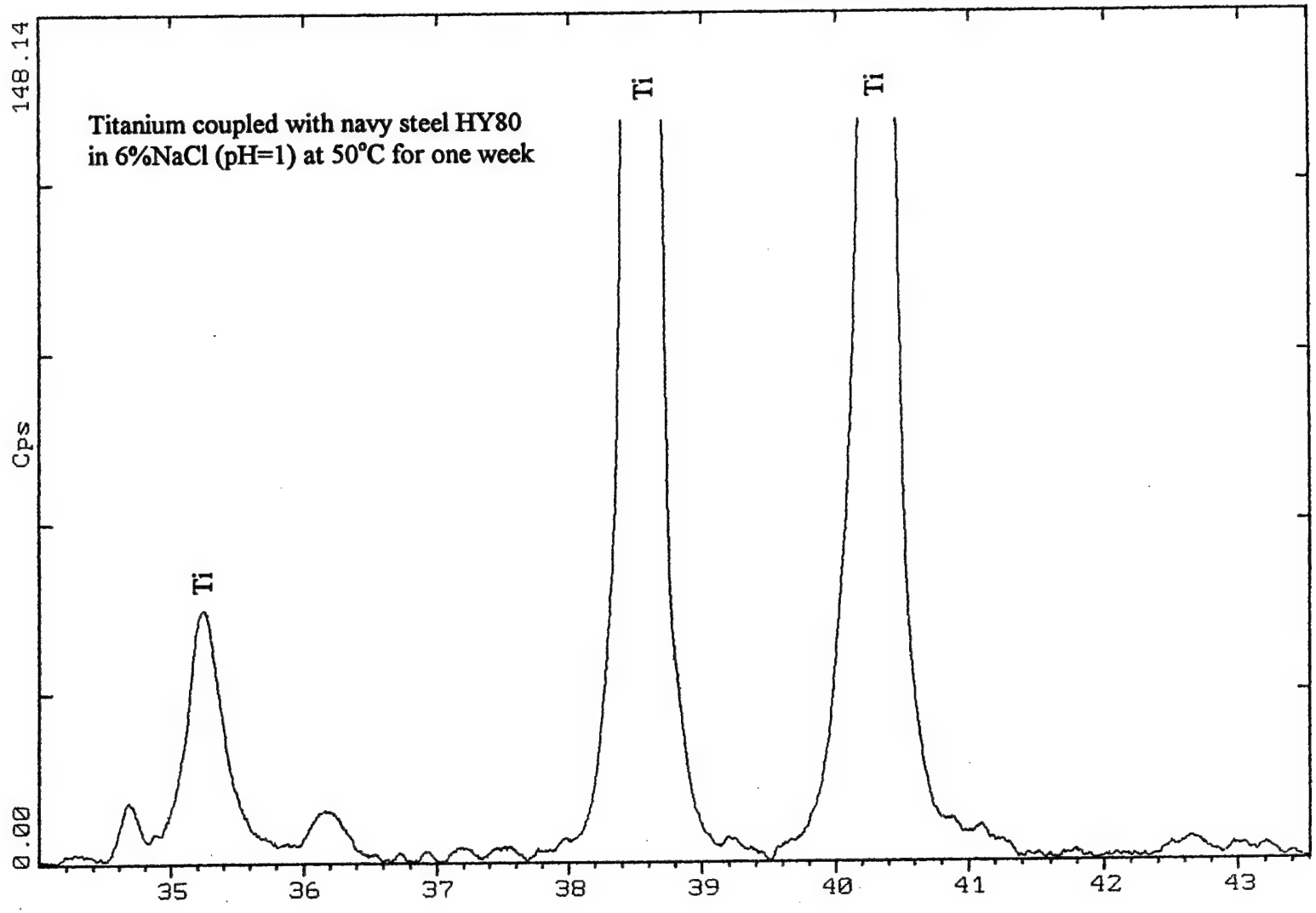

Figure 24 - XRD pattern obtained from titanium coupled HY80 sample after being exposed in 6%NaCl solution (pH=1) at 50°C for one week.

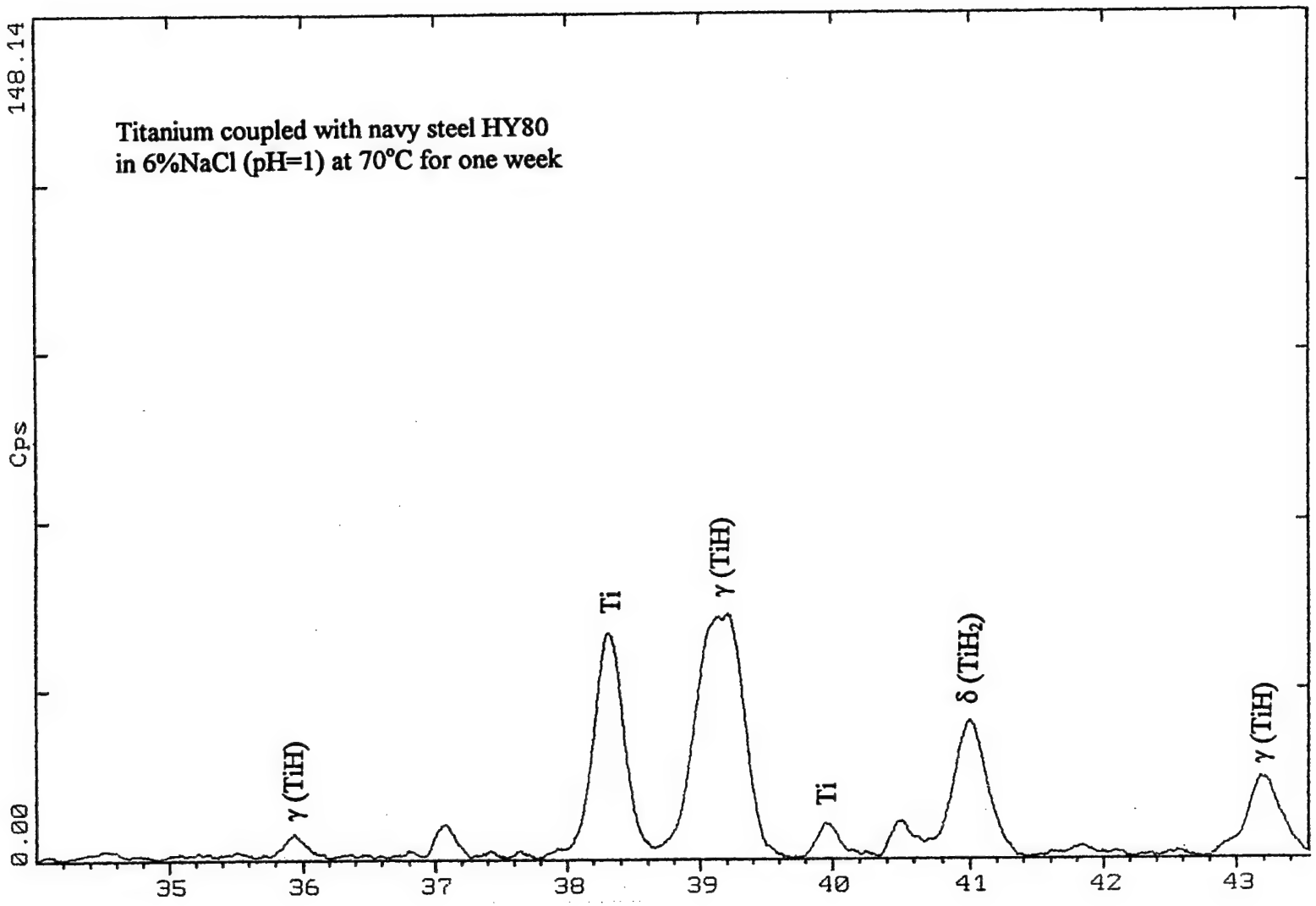

Figure 25 - XRD pattern obtained from titanium coupled HY80 sample after being exposed in 6%NaCl solution (pH=1) at 70°C for one week.

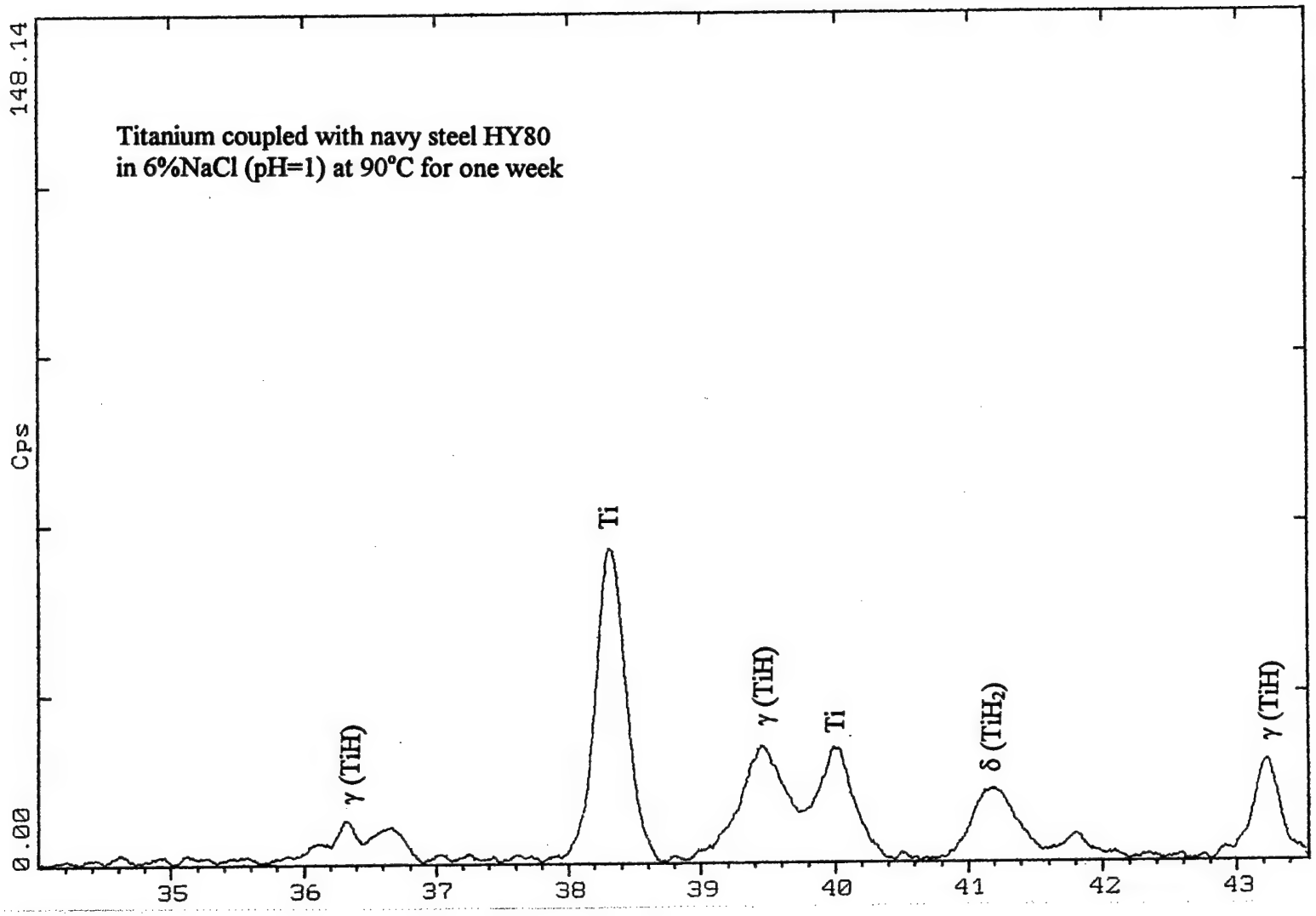

Figure 26 - XRD pattern obtained from titanium coupled HY80 sample after being exposed in 6%NaCl solution (pH=1) at 90°C for one week.

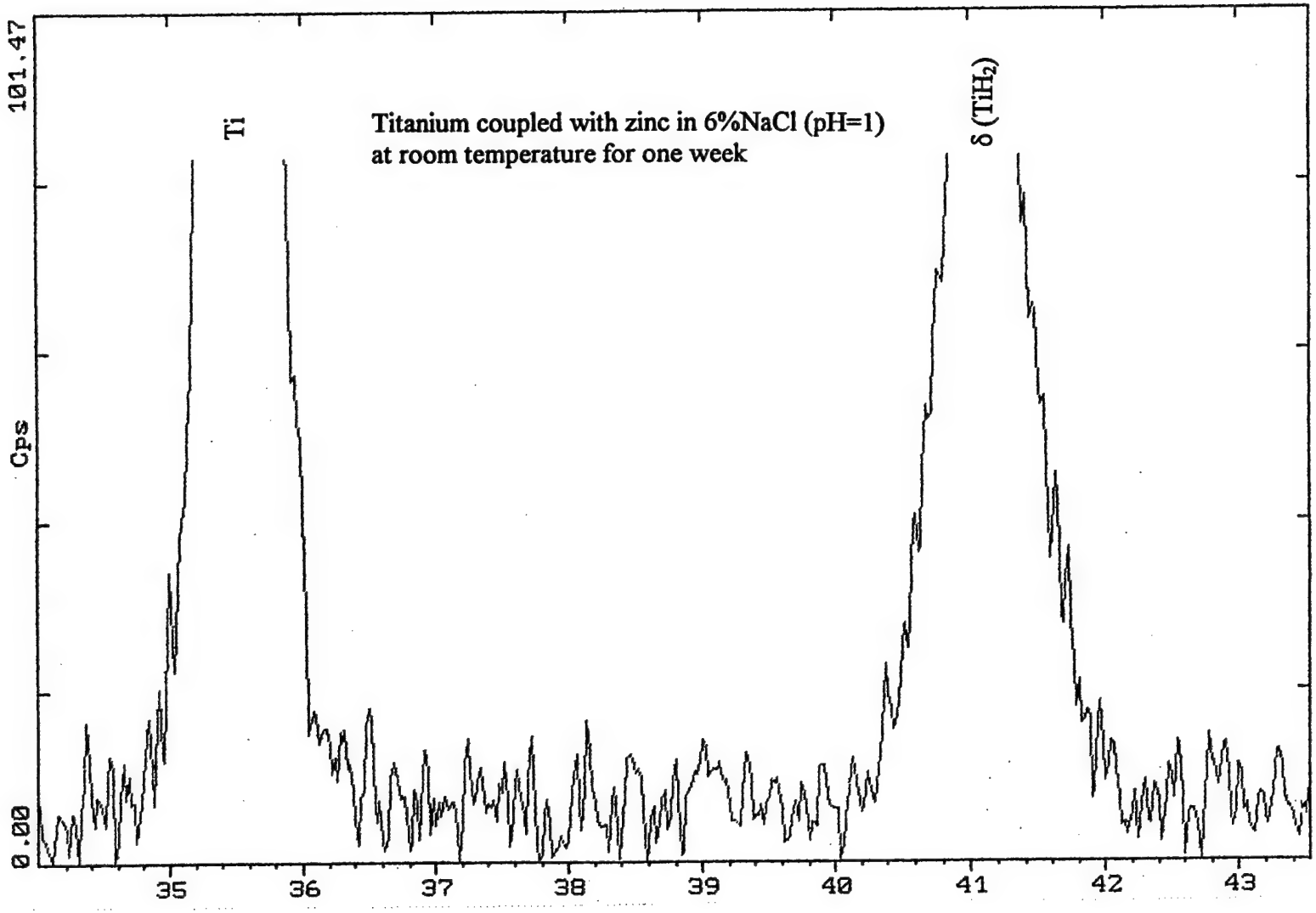

Figure 27 - XRD pattern obtained from titanium coupled zinc sample after being exposed in 6%NaCl solution (pH=1) at room temperature for one week.

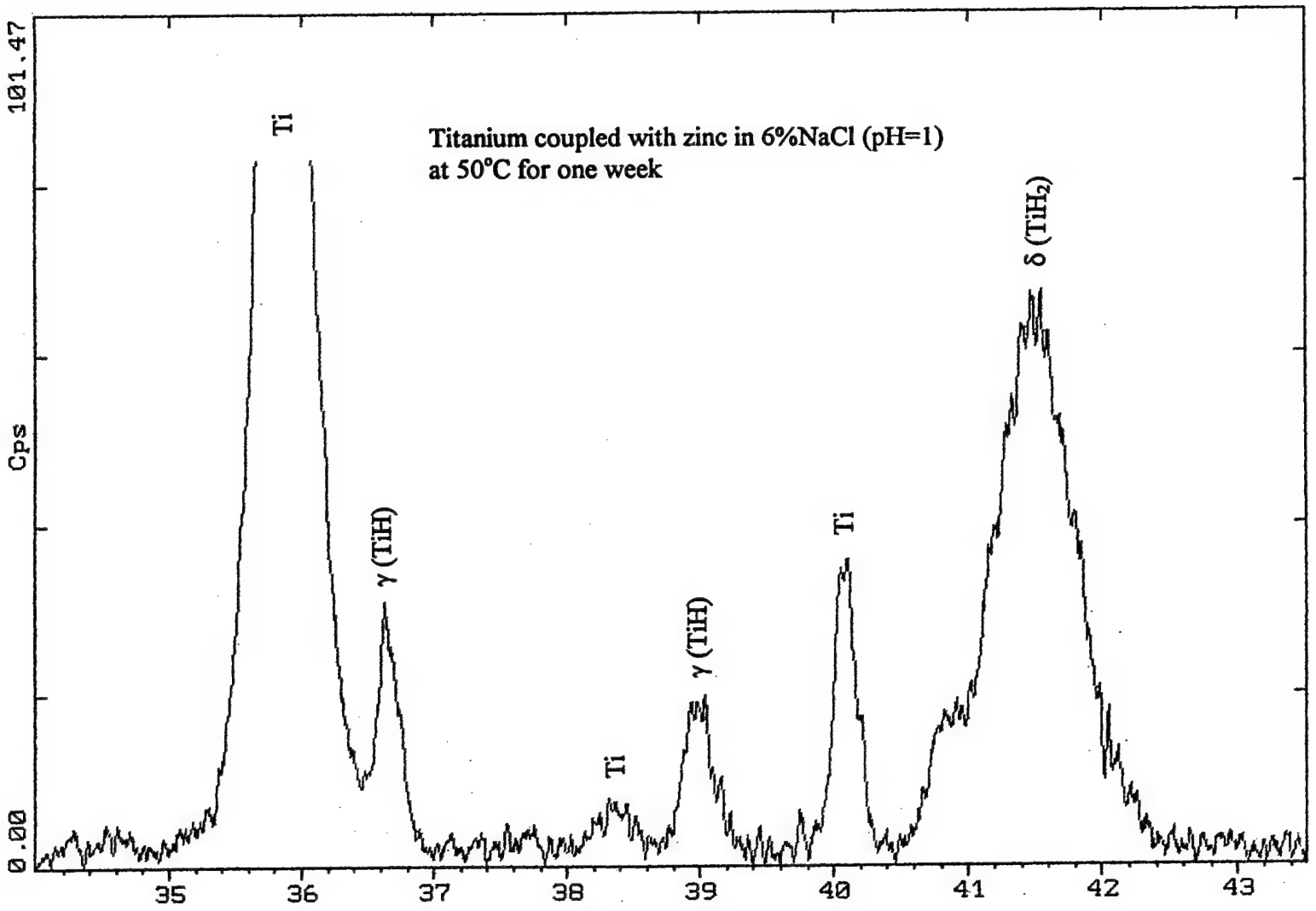

Figure 28 - XRD pattern obtained from titanium coupled zinc sample after being exposed in 6%NaCl solution (pH=1) at 50°C for one week.

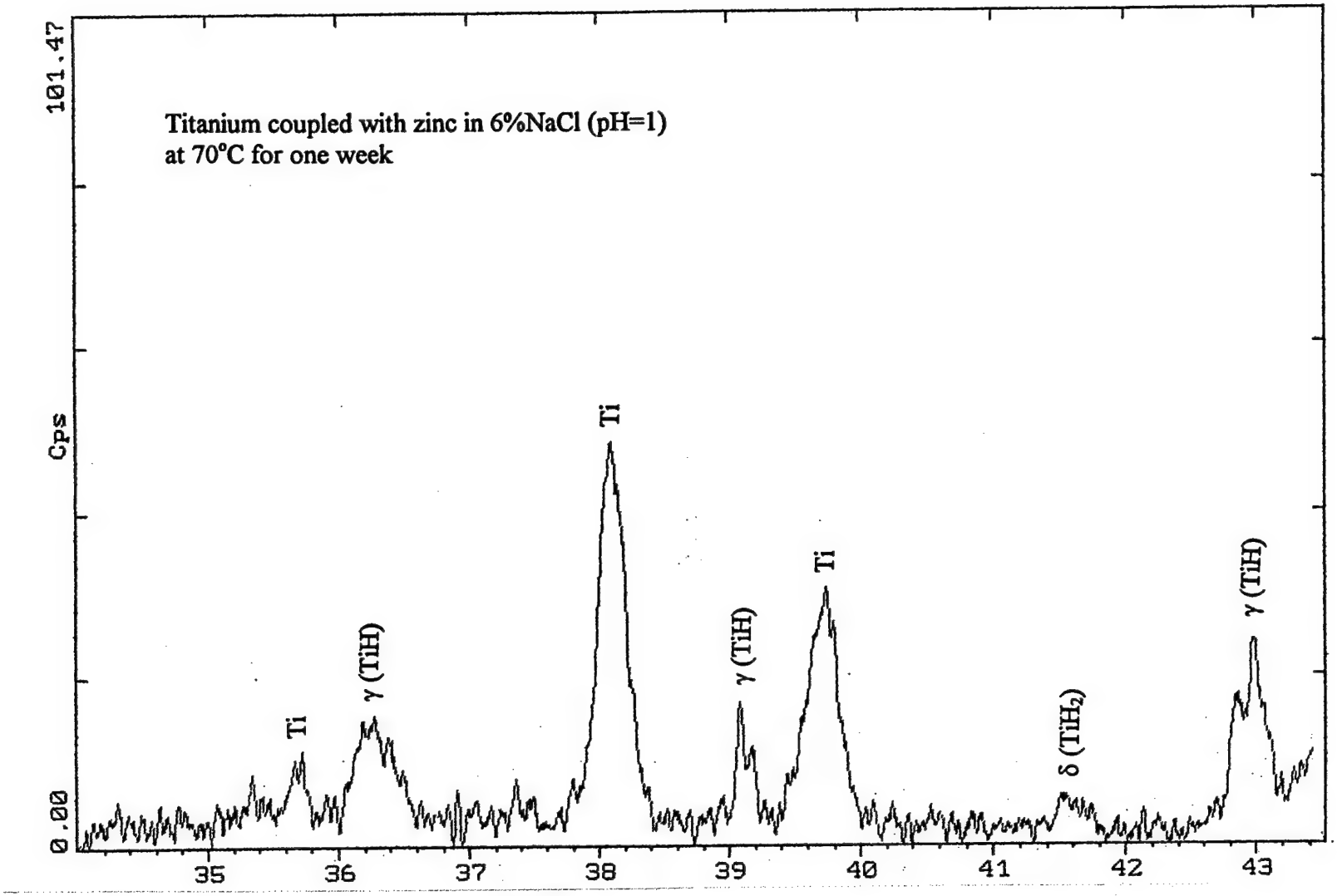

Figure 29 - XRD pattern obtained from titanium coupled zinc sample after being exposed in 6%NaCl solution (pH=1) at 70°C for one week.

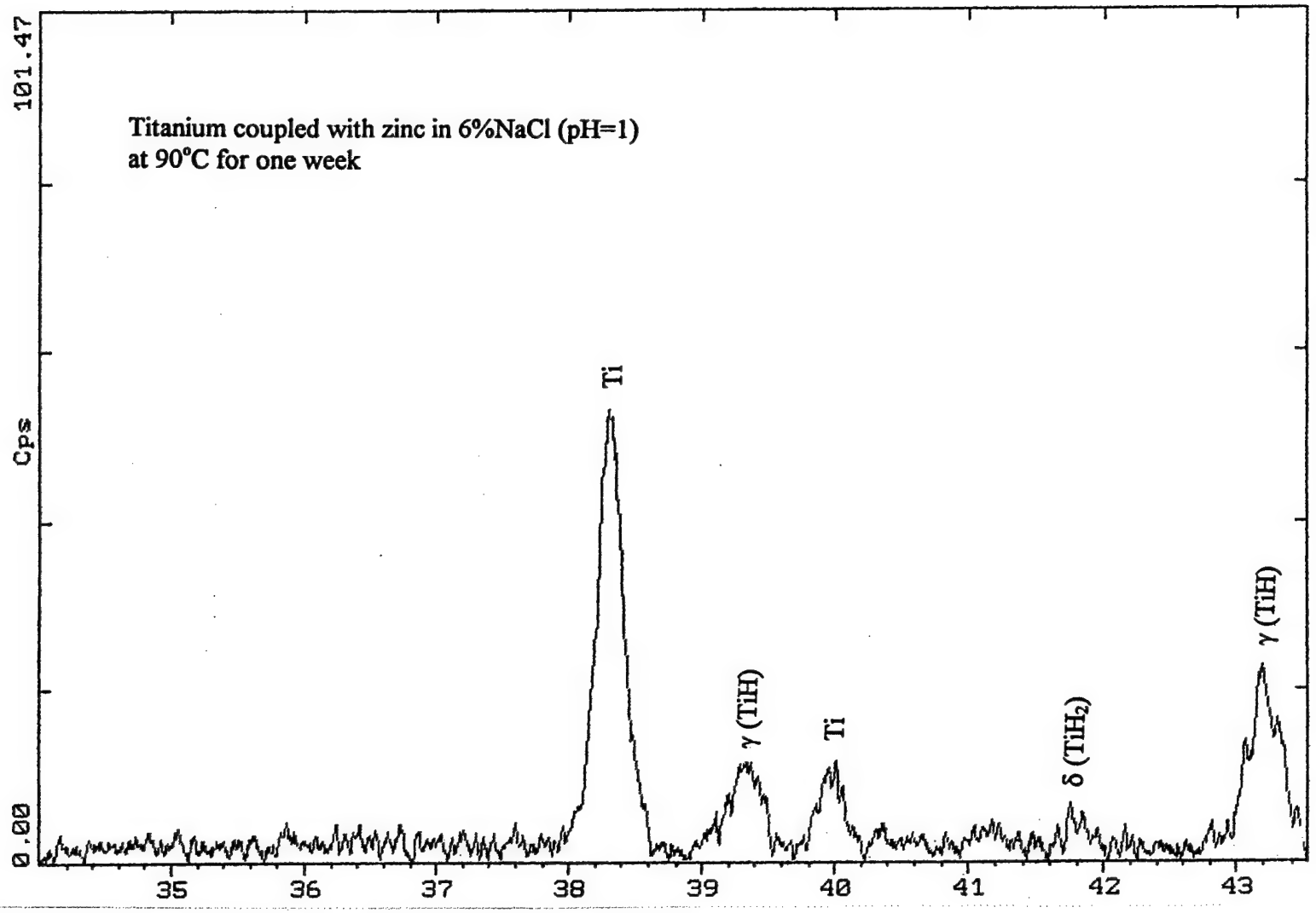

Figure 30 - XRD pattern obtained from titanium coupled zinc sample after being exposed in 6%NaCl solution (pH=1) at 90°C for one week.

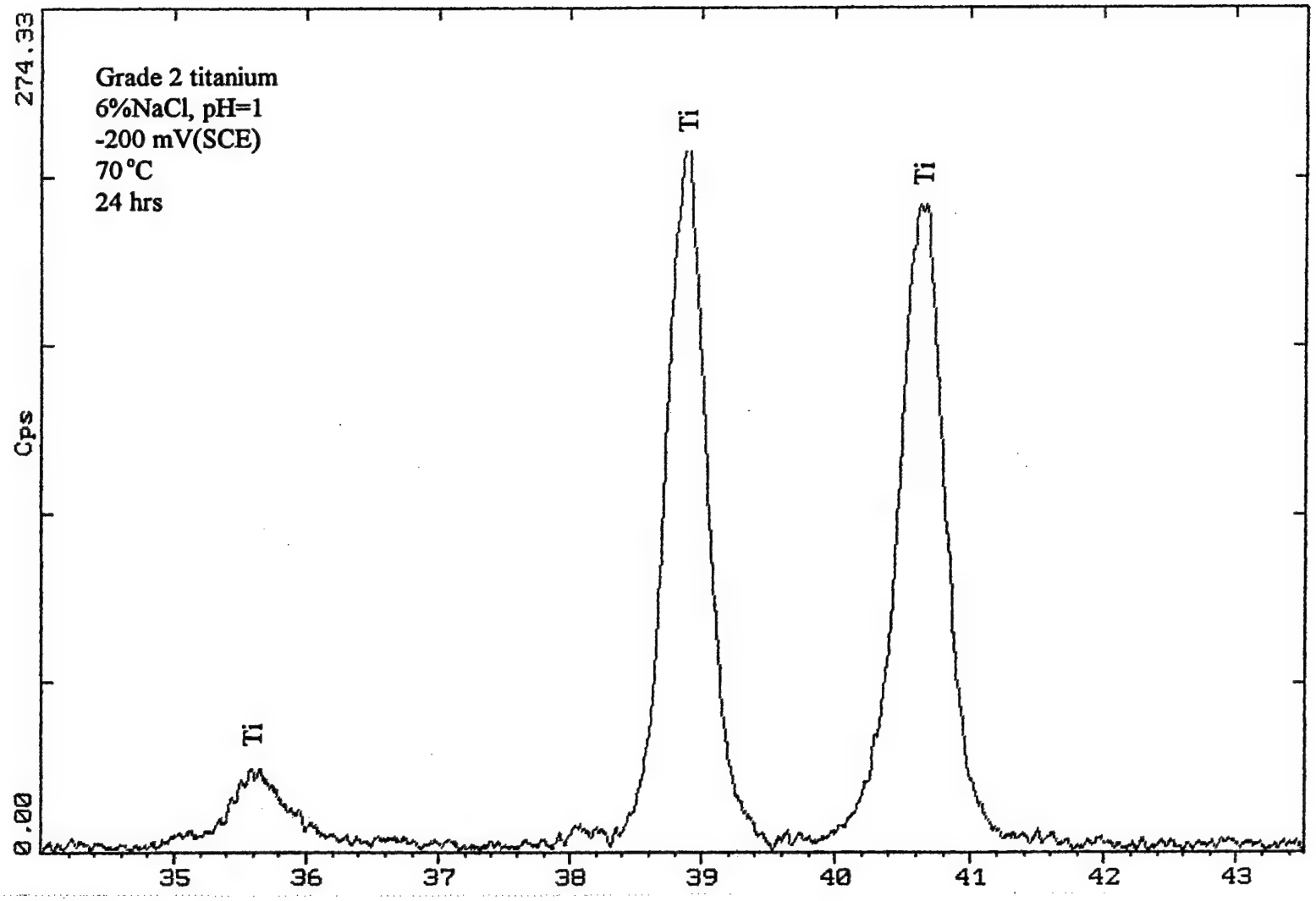

Figure 31 - XRD pattern obtained from sample after being charged at a potential of -200 mV_{SCE} in 6%NaCl solution (pH=1) at 70°C for 24 hours.

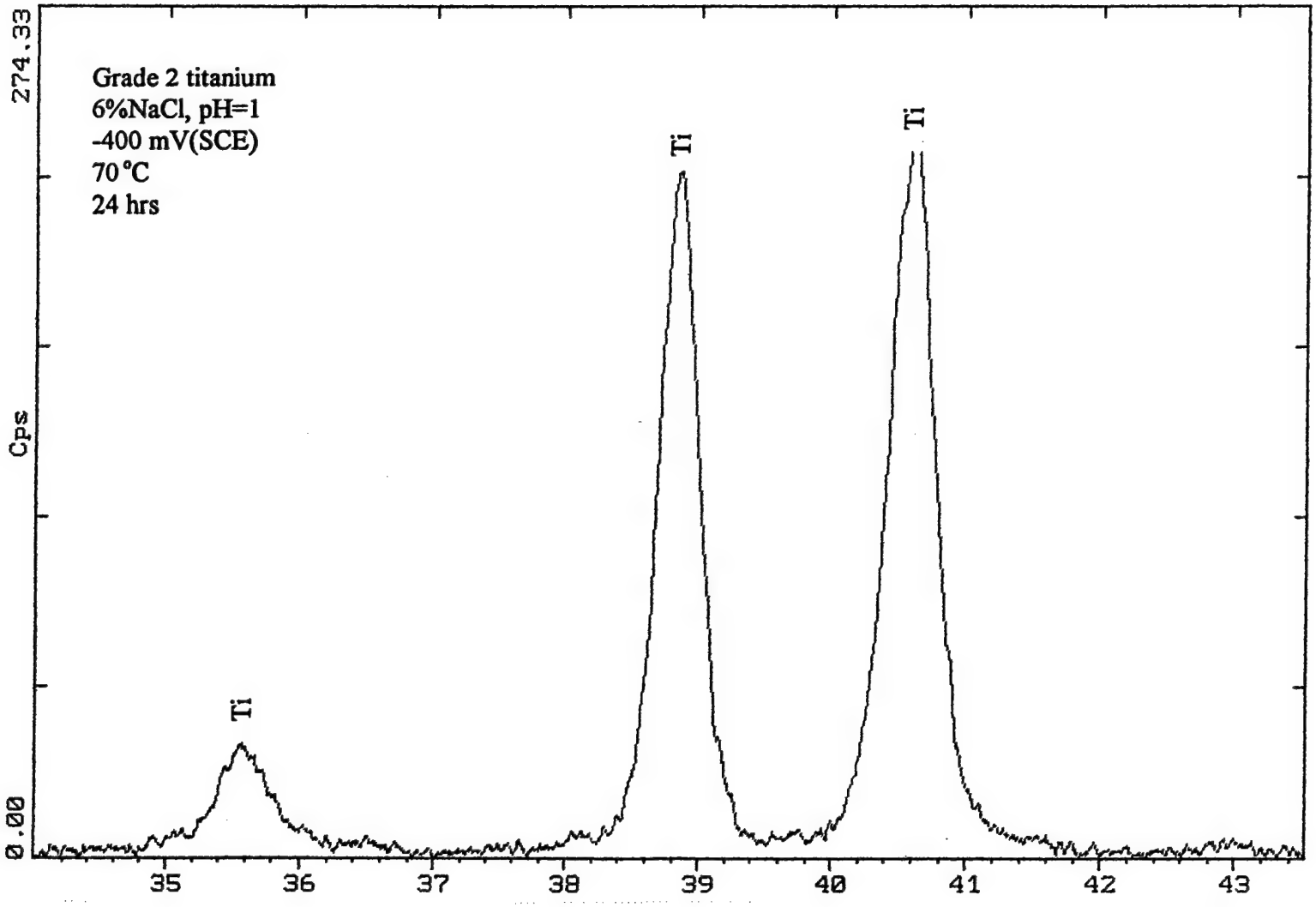

Figure 32 - XRD pattern obtained from sample after being charged at a potential of -400 mV_{SCE} in 6%NaCl solution (pH=1) at 70°C for 24 hours.

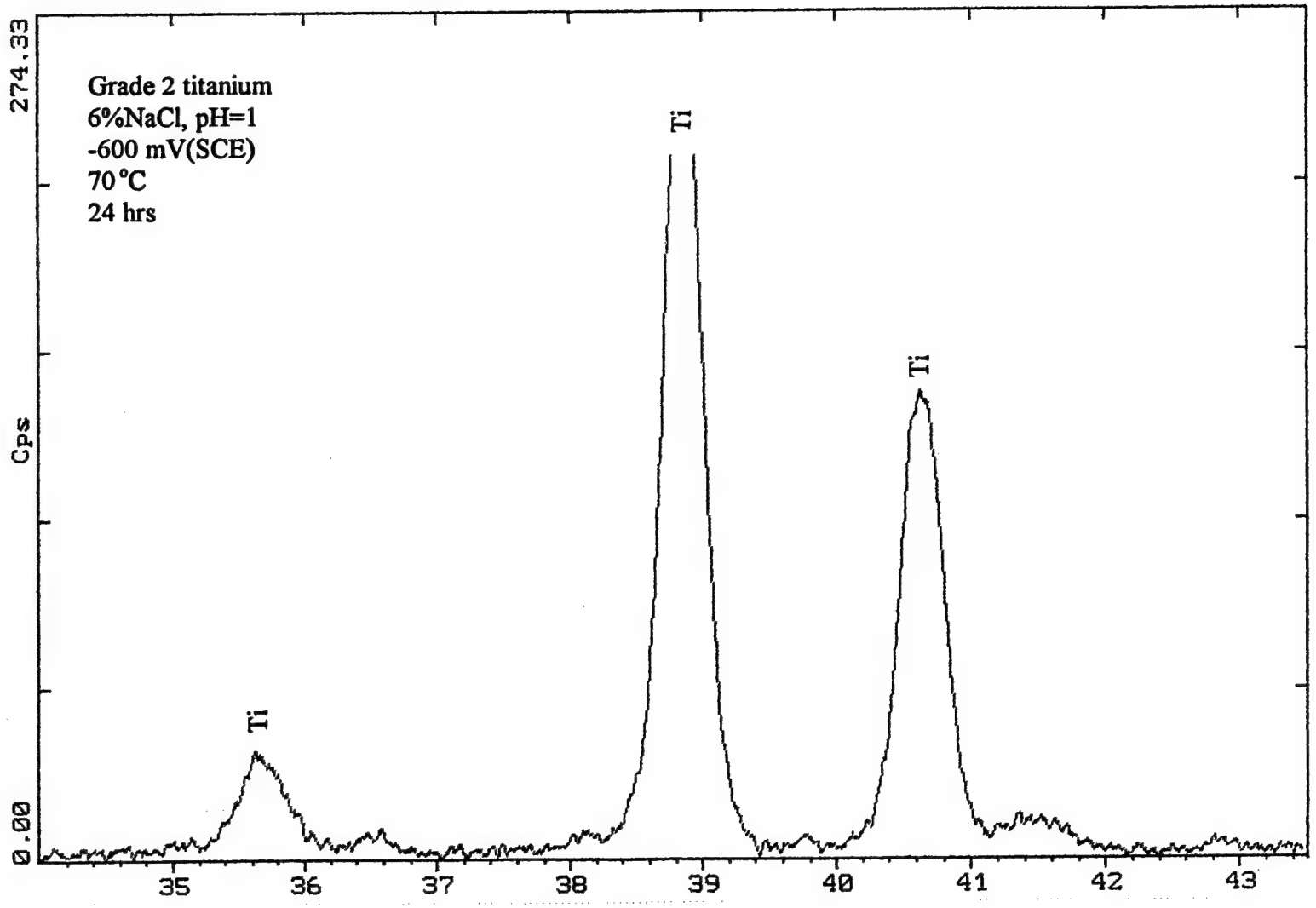

Figure 33 - XRD pattern obtained from sample after being charged at a potential of -600 mV_{SCE} in 6%NaCl solution (pH=1) at 70°C for 24 hours.

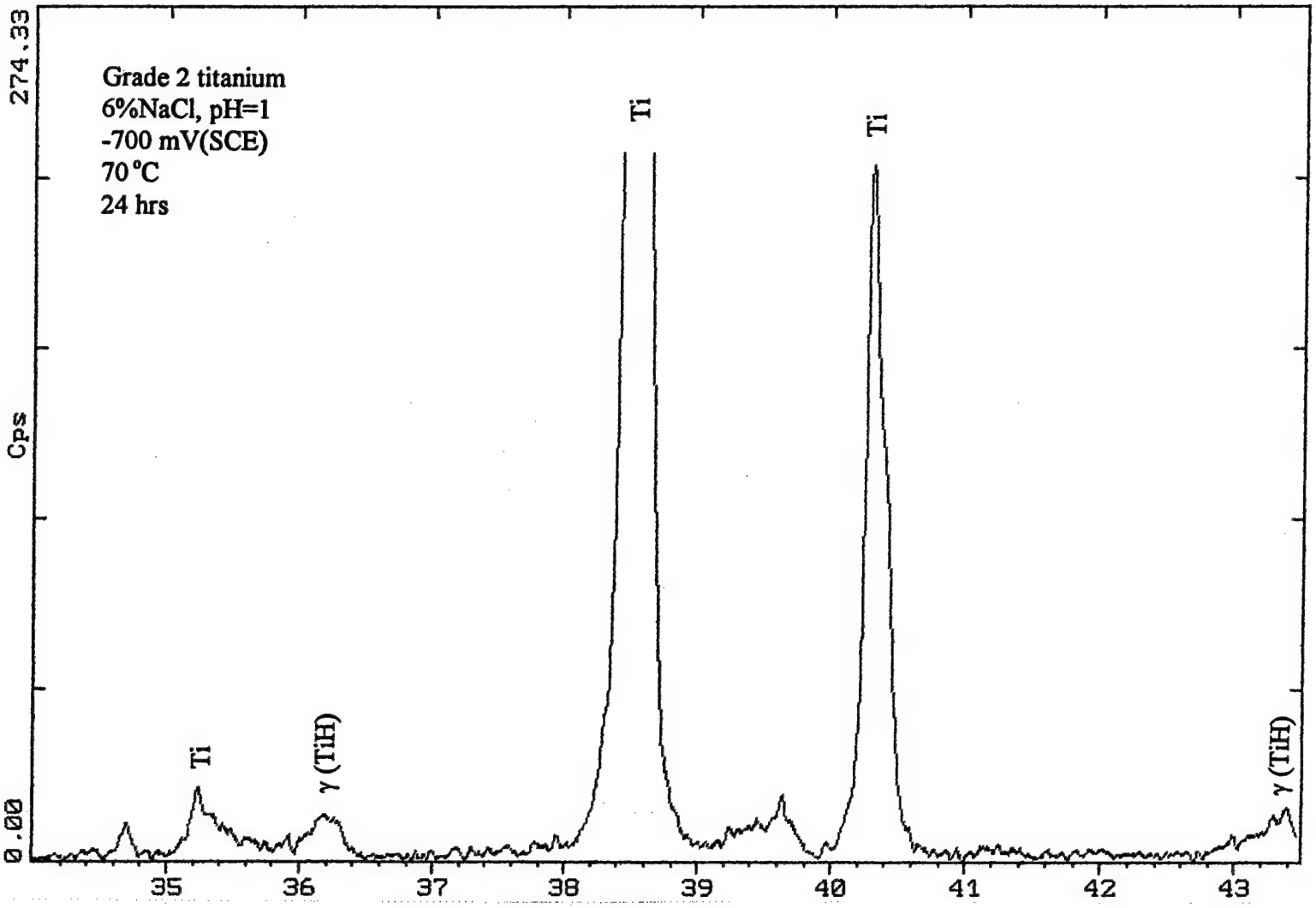

Figure 34 XRD pattern obtained from sample after being charged at a potential of -700 mV_{SCE} in 6%NaCl solution (pH=1) at 70°C for 24 hours.

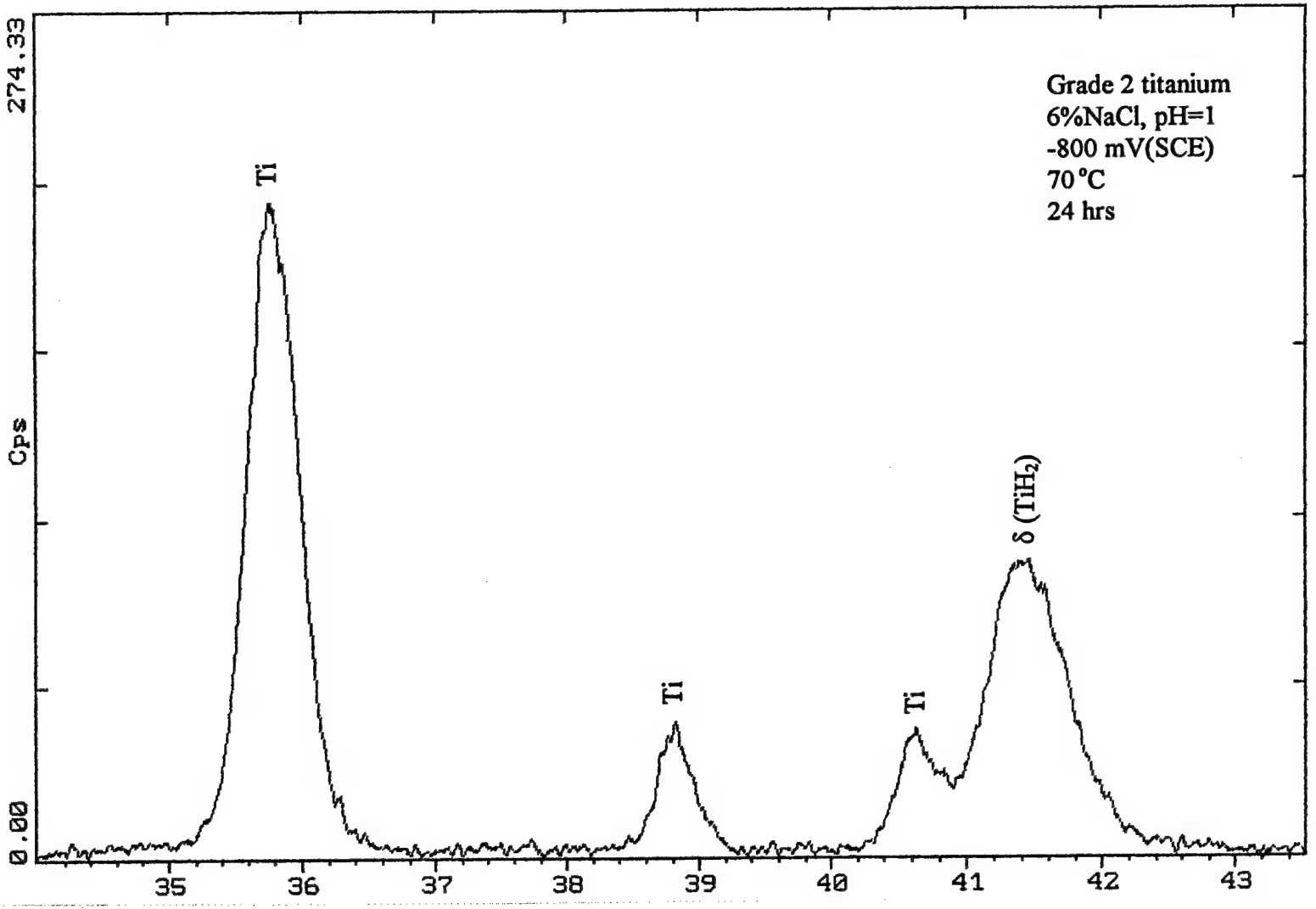

Figure 35 - XRD pattern obtained from sample after being charged at a potential of -800 mV_{SCE} in 6%NaCl solution (pH=1) at 70°C for 24 hours.

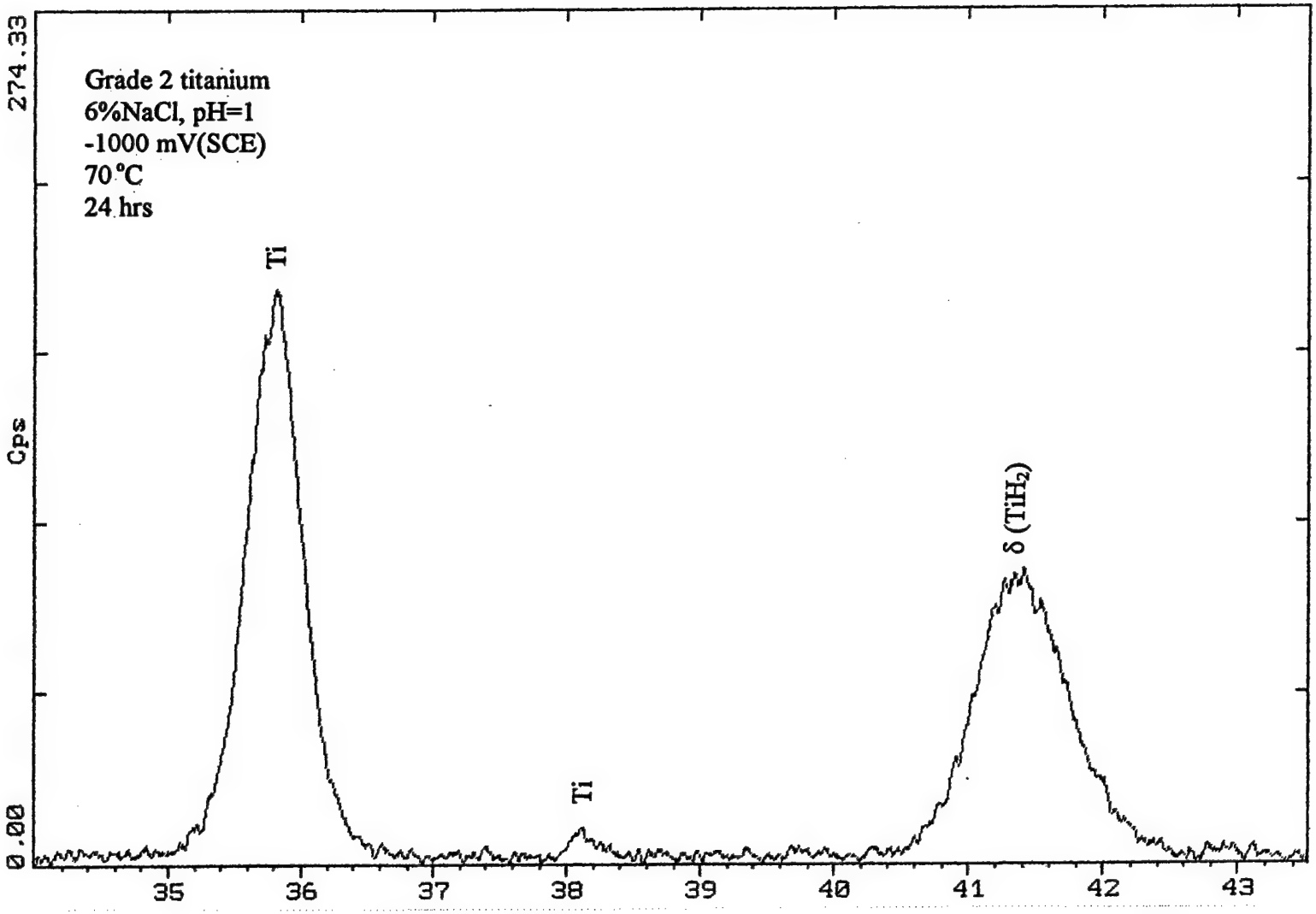

Figure 36 - XRD pattern obtained from sample after being charged at a potential of -1000 mV_{SCE} in 6%NaCl solution (pH=1) at 70°C for 24 hours.

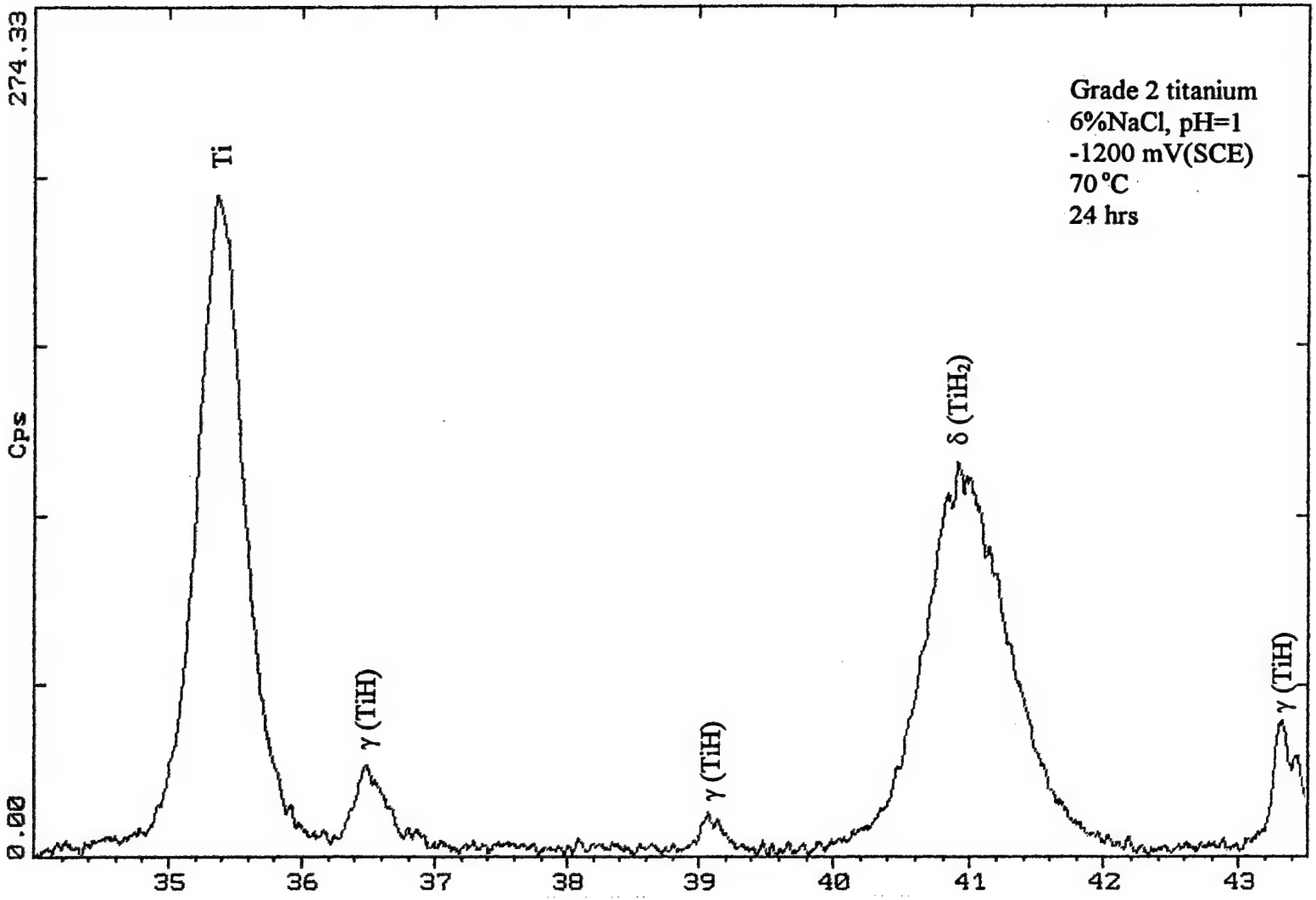

Figure 37 - XRD pattern obtained from sample after being charged at a potential of -1200 mV_{SCE} in 6%NaCl solution (pH=1) at 70°C for 24 hours.

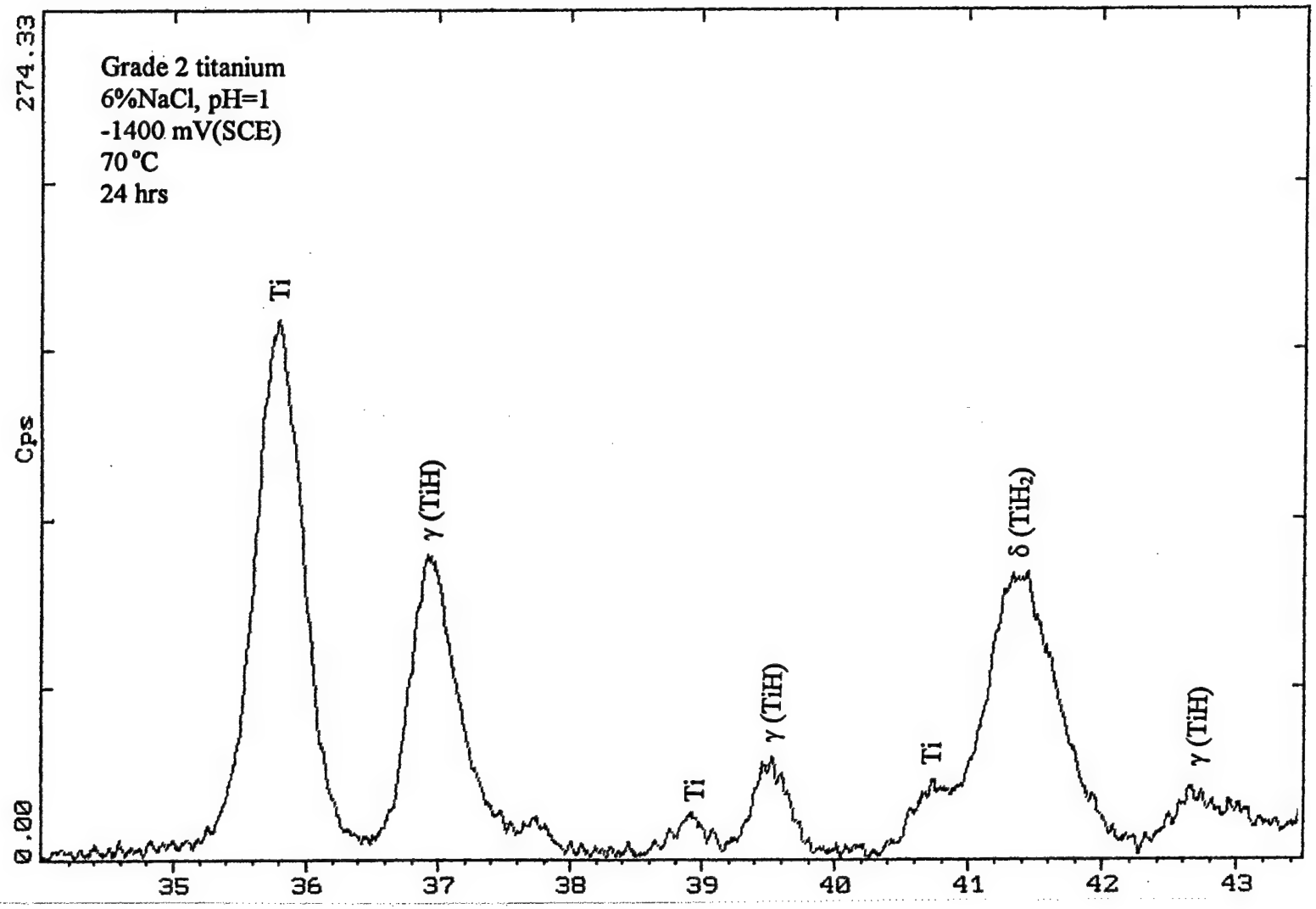

Figure 38 - XRD pattern obtained from sample after being charged at a potential of -1400 mV_{SCE} in 6%NaCl solution (pH=1) at 70°C for 24 hours.

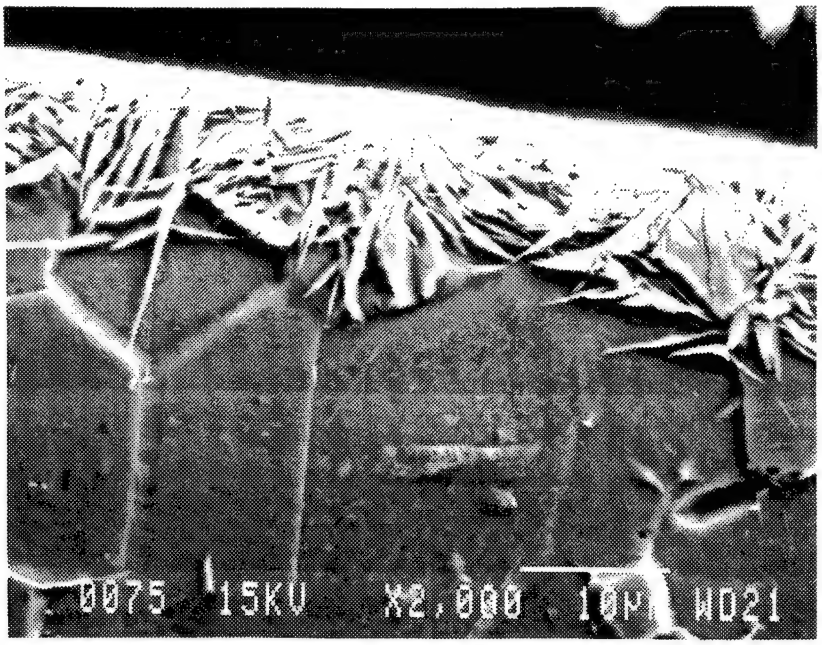

Figure 39 - Microstructure of hydride on the sample surface after the sample was charged in 6%NaCl solution with a current density of 0.5A/cm^2 for 12 hours.

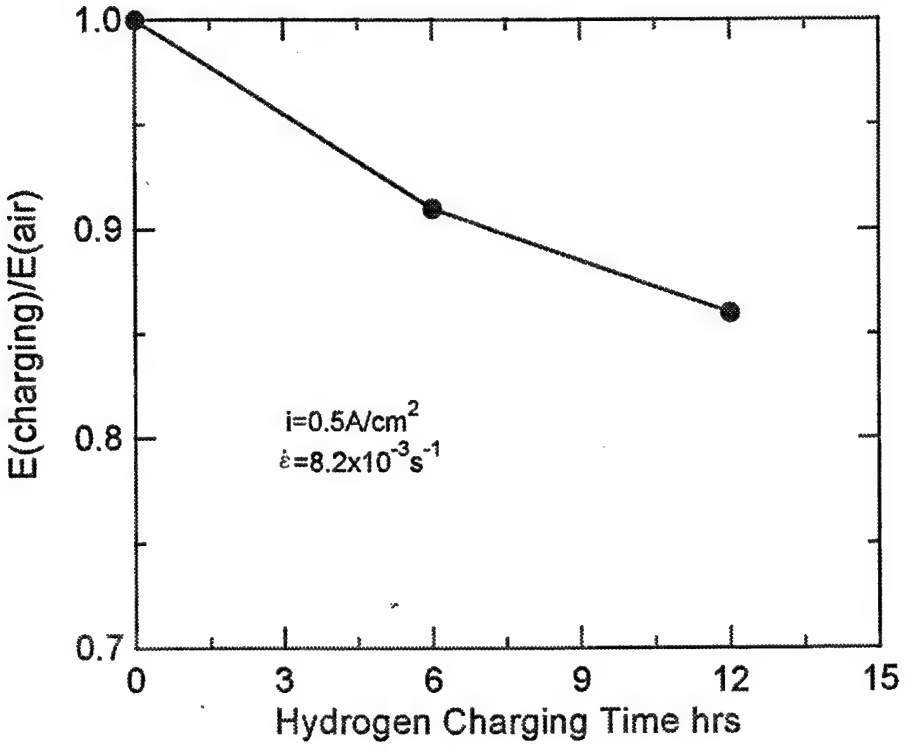

Figure 40 - Relationship between elongation loss and prior hydrogen charging time for smooth specimens (type A).

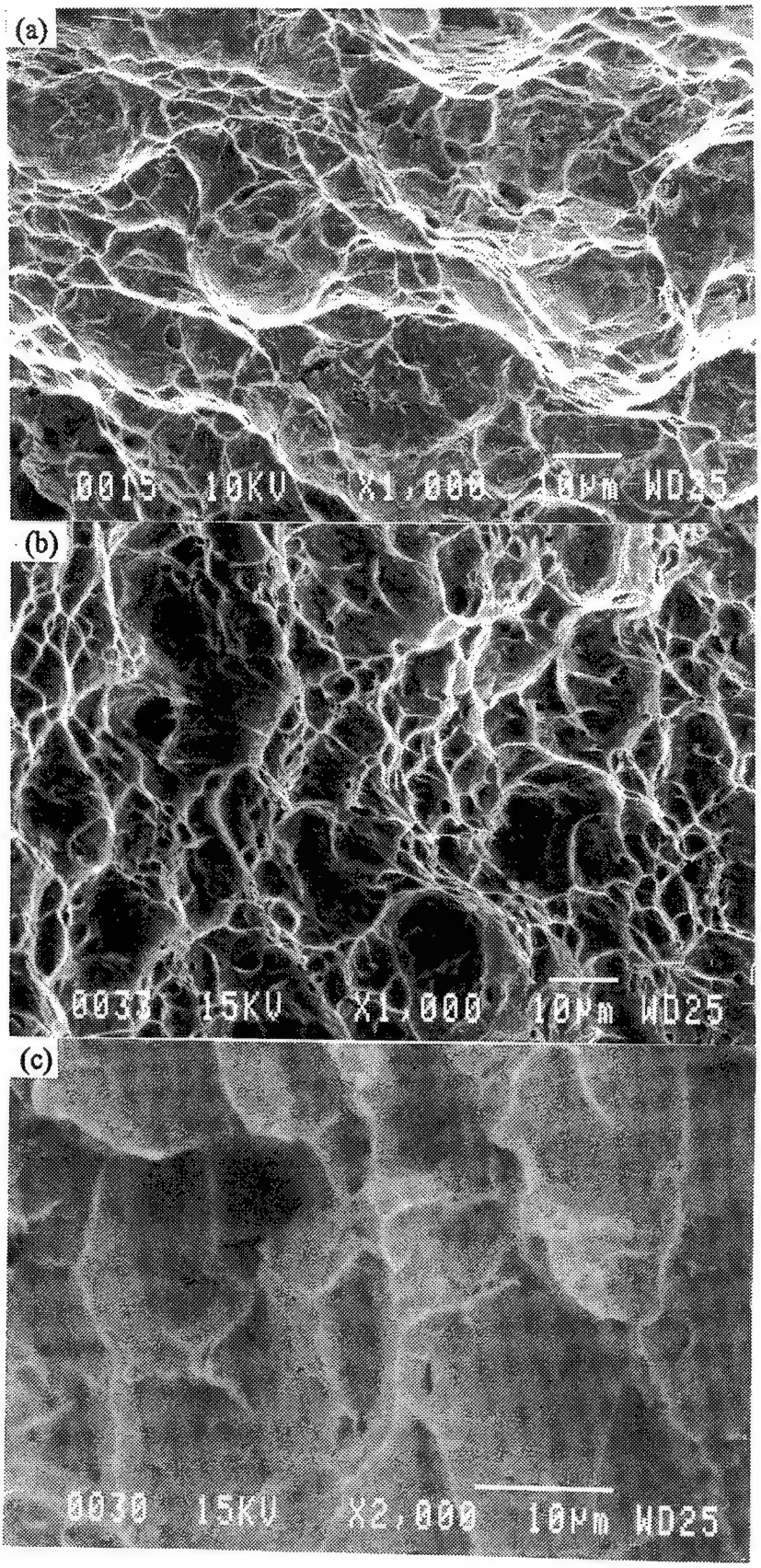

Figure 41 - Fracture surfaces for smooth specimens (type A) pulled to failure in air. (a) Uncharged (b) Center of sample charged for 12 hours. (c) Edge of sample charged for twelve hours.

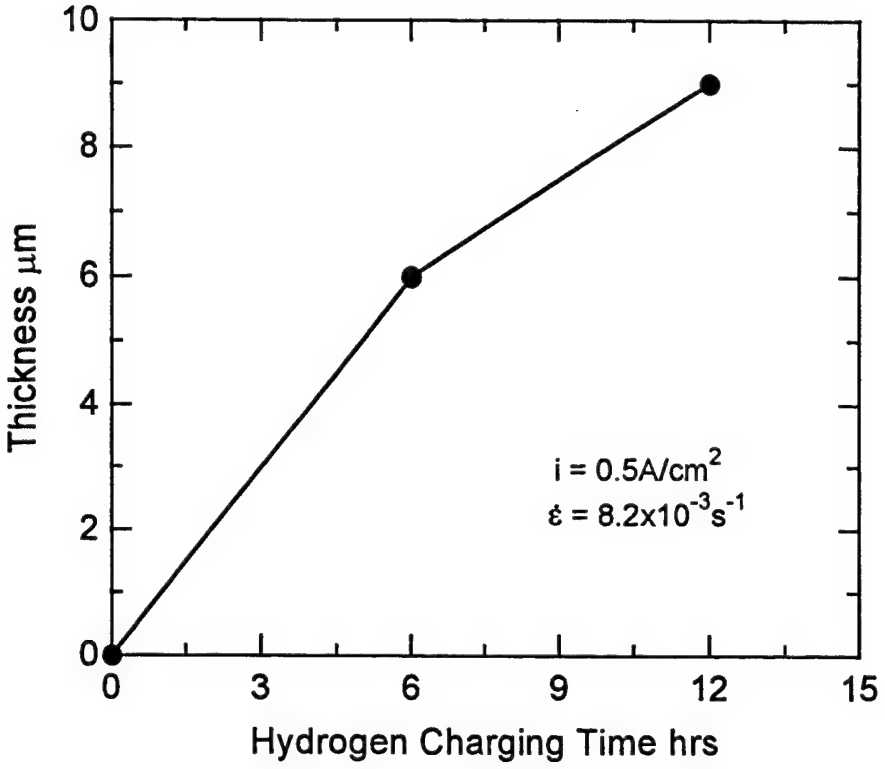

Figure 42 - Effect of hydrogen charging time on the thickness of the hydride layer on titanium sample surface.

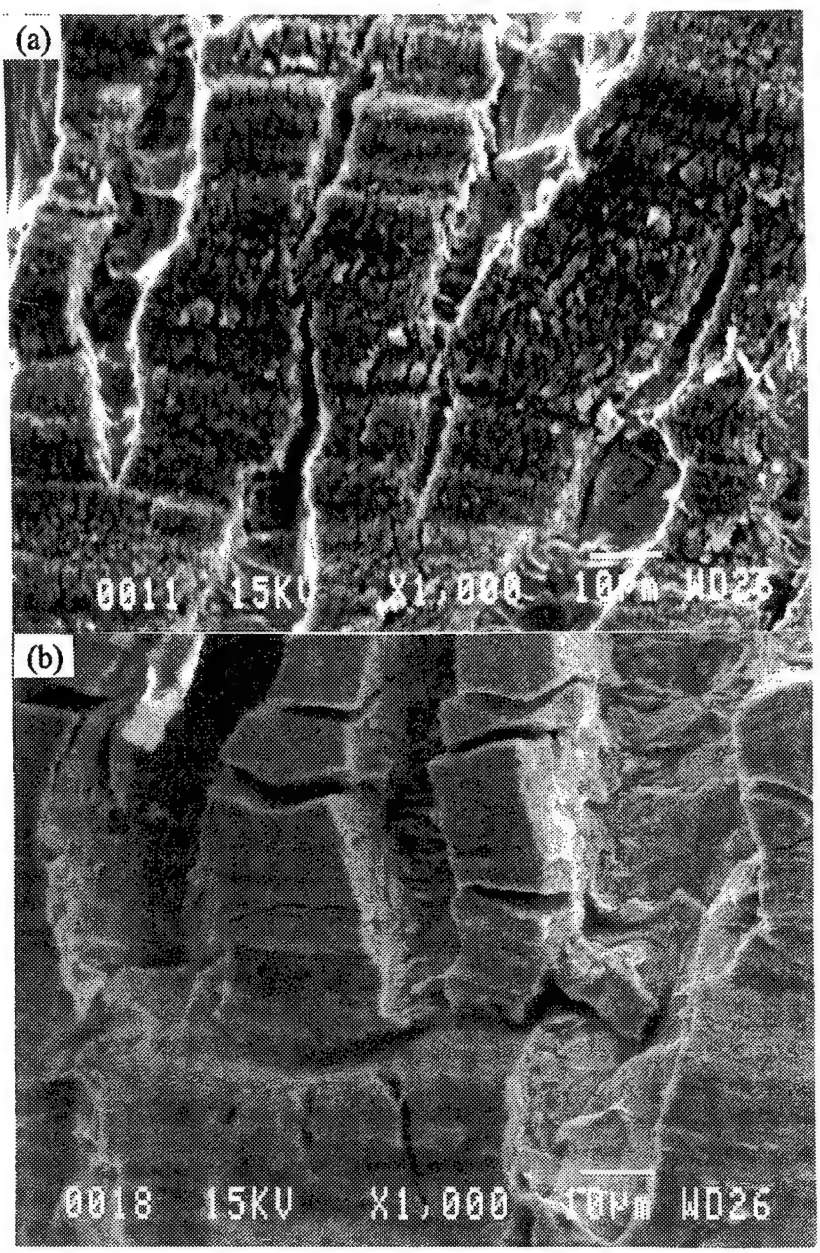

Figure 43 - Broken hydride layer observed on the sample surface after the material was pulled beyond the yield point. (a) Charged for 6 hours and (b) charged for 12 hours.

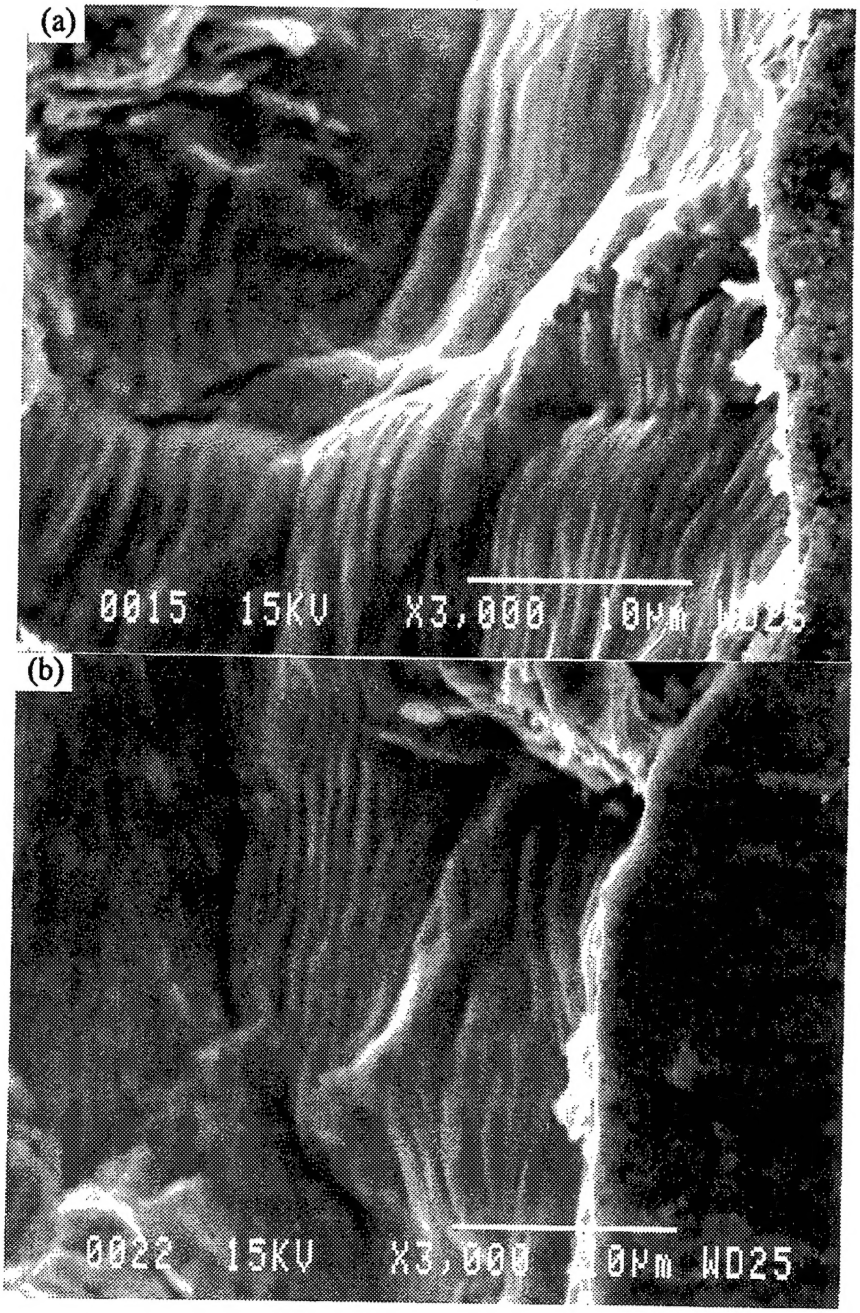

Figure 44 - Slip band appearance in the titanium underneath the broken hydride. (a) Sample charged for 6 hours and (b) sample charged for 12 hours.

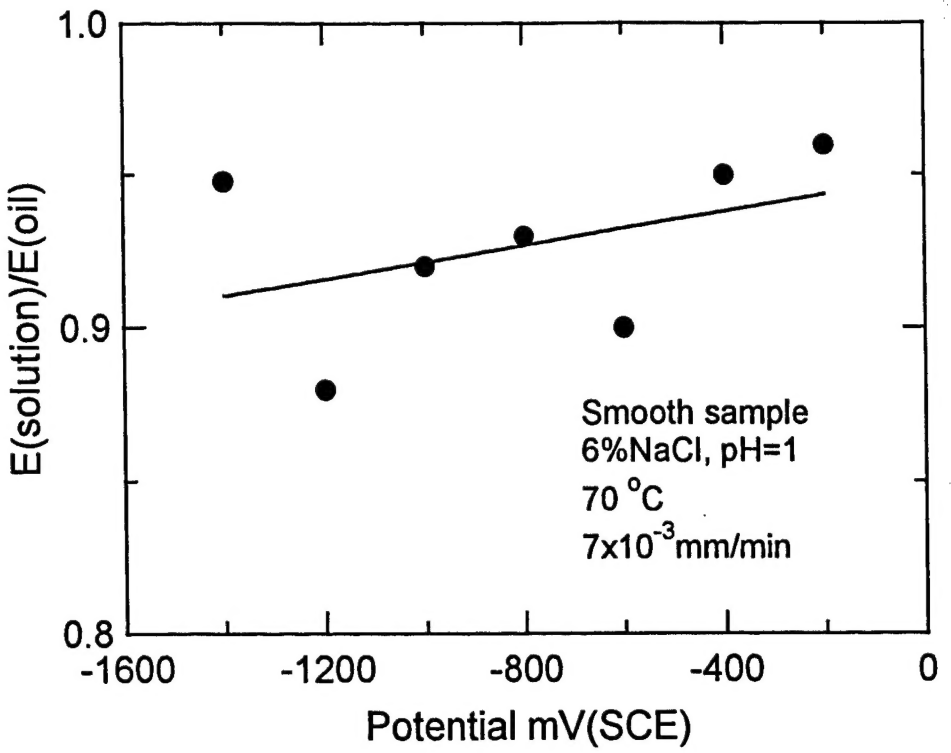

Figure 45 - The ratio of the elongation to failure in solution to that obtained in oil plotted as a function of applied potential.

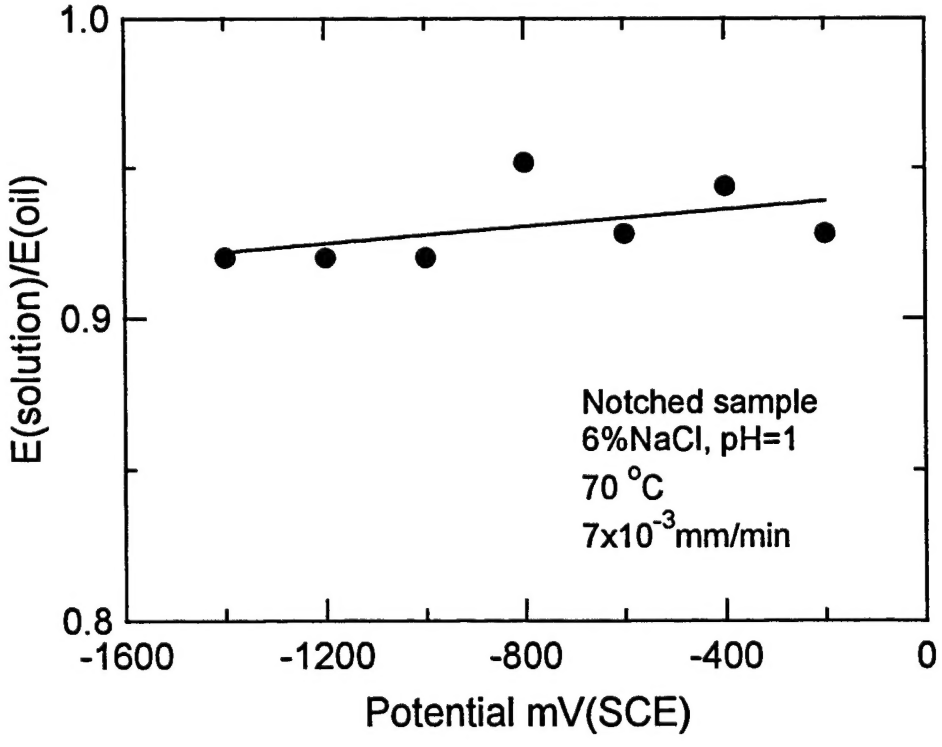

Figure 46 - The ratio of the elongation to failure in solution to that obtained in oil for notched samples as a function of applied potential.

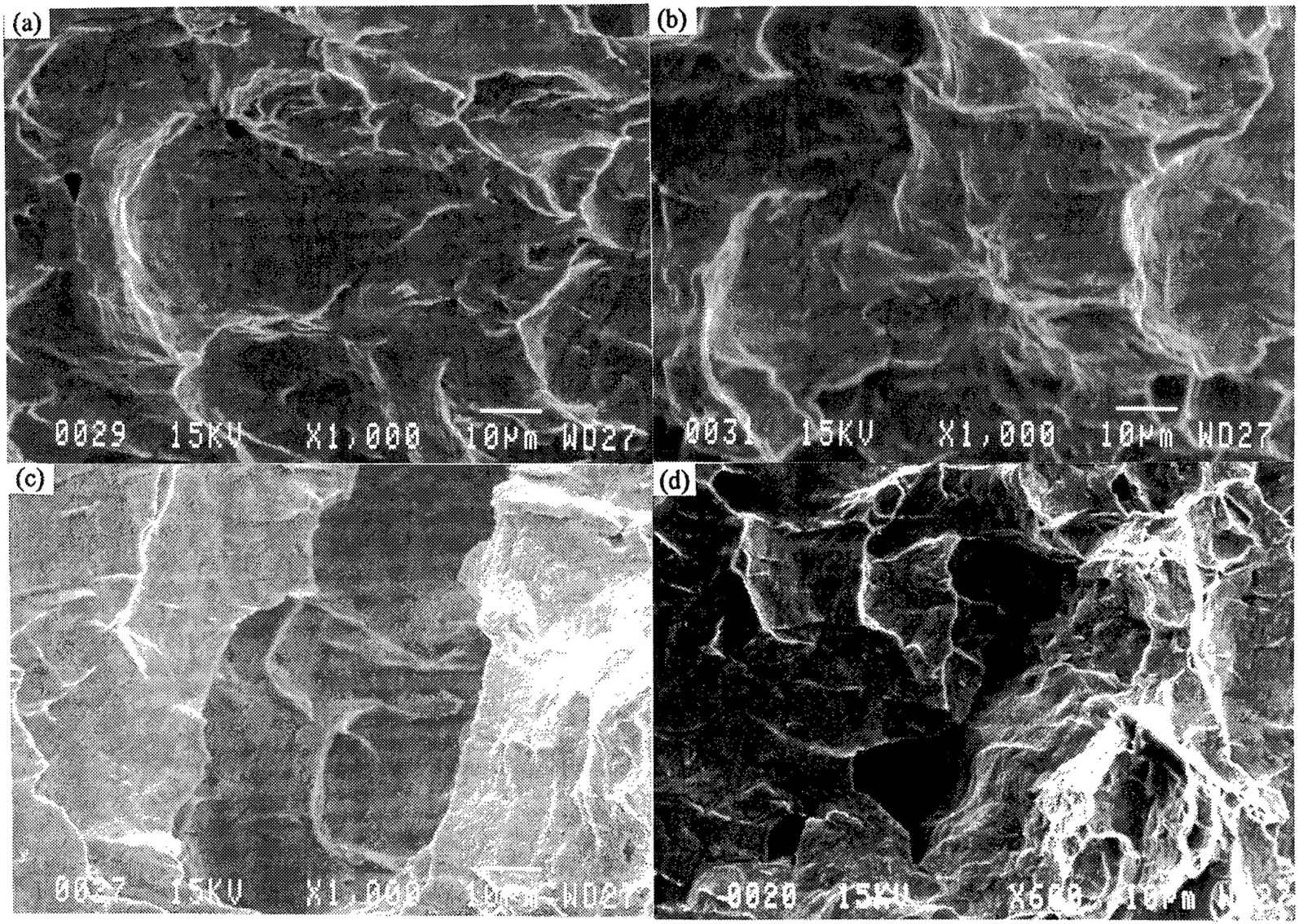

Figure 47 - Fracture surfaces for notched samples tested in tension to failure at 70°C. (a.) Tested in oil. (b.) Tested in 6%NaCl solution (pH=1) at an applied potential of -800 mV_{SCE}, (c) -1000 mV_{SCE} and (d) -1200 mV_{SCE}

REPORT DOCUMENTATION PAGE

Form Approved
OMB No. 0704-0188

Public reporting burden for this collection of information is estimated to average 1 hour per response, including the time for reviewing instructions, searching existing data sources, gathering and maintaining the data needed, and completing and reviewing the collection of information. Send comments regarding this burden estimate or any other aspect of this collection of information, including suggestions for reducing this burden, to Washington Headquarters Services, Directorate for Information Operations and Reports, 1215 Jefferson Davis Highway, Suite 1204, Arlington, VA 22202-4302, and to the Office of Management and Budget, Paperwork Reduction Project (0704-0188), Washington, DC 20503.

1. AGENCY USE ONLY (Leave blank)	2. REPORT DATE	3. REPORT TYPE AND DATES COVERED
	March 1997	First Annual Report (1996)

4. TITLE AND SUBTITLE

Hydriding of Titanium

5. FUNDING NUMBERS

Grant No.
N00014-96-1-0272

6. AUTHOR(S)

Clyde L. Briant, K. Sharvan Kumar, Zhengfu Wang

7. PERFORMING ORGANIZATION NAME(S) AND ADDRESS(ES)

Division of Engineering
Brown University
Box D, 182 Hope Street
Providence, RI 02912-9104

8. PERFORMING ORGANIZATION REPORT NUMBER

None

9. SPONSORING/MONITORING AGENCY NAME(S) AND ADDRESS(ES)

Office of Naval Research
800 N. Quincy Street
Arlington, VA 22217-5660

10. SPONSORING/MONITORING AGENCY REPORT NUMBER

11. SUPPLEMENTARY NOTES

None

12a. DISTRIBUTION/AVAILABILITY STATEMENT

Approved for public release; any or all parts of this document may be reproduced for use by U.S. Government

12b. DISTRIBUTION CODE

13. ABSTRACT *(Maximum 200 words)*

The work reported in this document addresses research on hydride formation in grade II titanium when it is exposed to sea water and the effect of this exposure on its mechanical properties. The results that we have obtained generally verify the previously reported good response of grade II titanium when exposed to this environment. Hydrides can form on the surface of the sample at potentials below approximately -600mV_{SCE}. However, these hydrides do not seriously degrade the mechanical properties of this material, and the samples showed good ductility even for tests run at electrochemical potentials as low as -1400 mV_{SCE}. When a thick hydride layer was formed on the surface by extreme cathodic charging, only a small decrease in elongation could be observed; even though the brittle film cracked, the underlying metal was ductile. An increase in temperature and a decrease in pH increased the electrochemical potential of the titanium. Galvanic coupling experiments showed that hydrides formed in titanium coupled to zinc and aluminum at all temperatures between 23 and 90°C. The reaction with zinc was so extreme that the zinc dissolved from the couple. When the titanium was coupled to HY80 steel, hydrides formed when the temperature exceeded 70°C. It would appear, based on the above results, that the main concern would be applications where galvanic coupling might occur between the Navy steel HY80 and grade II titanium.

14. SUBJECT TERMS

Titanium, hydrides, corrosion, galvanic corrosion, sea water

15. NUMBER OF PAGES

72

16. PRICE CODE

17. SECURITY CLASSIFICATION OF REPORT	18. SECURITY CLASSIFICATION OF THIS PAGE	19. SECURITY CLASSIFICATION OF ABSTRACT	20. LIMITATION OF ABSTRACT
unclassified	unclassified	unclassified	unlimited